AD-A151 450 WATER WAVE PROPAGATION OVER UNEVEN BOTTOMS(U) FLORIDA UNIV GAINESVILLE DEPT OF COASTAL AND OCEANOGRAPHIC ENGINEERING J T KIRBY JAN 85 UFL/COEL-TR/055 1/1

UNCLASSIFIED N00014-84-C-0188 F/G 20/4 NL

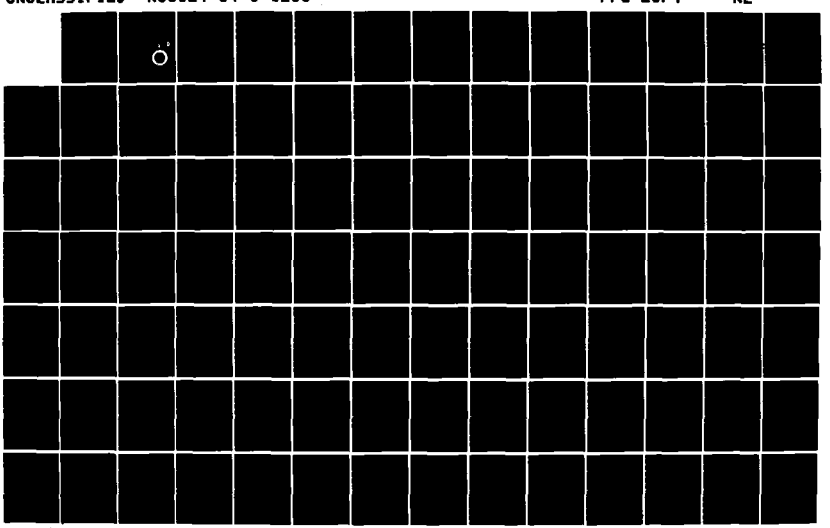

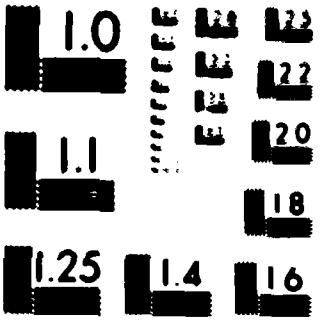
1.0
1.1
1.25
1.4
1.6
2.2
2.0
1.8

UFL/COEL-TR/055

WATER WAVE PROPAGATION OVER UNEVEN BOTTOMS

BY

JAMES T. KIRBY

JANUARY 1985

COASTAL & OCEANOGRAPHIC ENGINEERING DEPARTMENT
UNIVERSITY OF FLORIDA
Gainesville, Florida 32611

REPORT DOCUMENTATION PAGE

1. Report No.	2. AD A151 452	3. Recipient's accession no
4. Title and Subtitle: Water Wave Propagation Over Uneven Bottoms		5. Report Date: January 1985
7. Author(s): James T. Kirby		8. Performing Organization Report No: UFL/COEL-TR/055
9. Performing Organization Name and Address: Coastal and Oceanographic Engineering Department, University of Florida, 336 Weil Hall, Gainesville, FL 32611		10. Project/Task/Work Unit No.
		11. Contract or Grant No: N00014-84-C-0188
12. Sponsoring Organization Name and Address: Office of Naval Research, Arlington, VA subcontract through University of Delaware, Newark, DE 19716		13. Type of Report: Technical
15. Supplementary Notes		

16. Abstract

This report consists of two parts. In Part 1, a time dependent form of the reduced wave equation of Berkhoff is developed for the case of waves propagating over a bed consisting of ripples superimposed on an otherwise slowly varying mean depth which satisfies the mild slope assumption. The ripples are assumed to have wavelengths on the order of the surface wave length but amplitudes which scale as a small parameter along with the bottom slope. The theory is verified by showing that it reduces to the case of plane waves propagating over a one-dimensional, infinite patch of sinusoidal ripples, studied recently by Davies and Heathershaw and Mei. We then study two cases of interest; formulation and use of the coupled parabolic equations for propagation over patches of arbitrary form in order to study wave reflection, and propagation of trapped waves along an infinite ripple patch.

In the second part, we use the results of Part 1 to extend the results for weakly-nonlinear wave propagation to the case of partial reflection from bottoms with mild-sloping mean depth with superposed small amplitude undulations.

17. Originator's Key Words	18. Availability Statement		
Combined refraction-diffraction Water waves Wave reflection	distribution unlimited		
19. U. S. Security Classif. of the Report: unclassified	20. U. S. Security Classif. of This Page: unclassified	21. No. of Pages: 95	22. Price

UFL/COEL-TR/055

WATER WAVE PROPAGATION OVER UNEVEN BOTTOMS

by

JAMES T. KIRBY

Coastal and Oceanographic Engineering Department

University of Florida, Gainesville, FL 32611

Technical Report to the Office of Naval Research,

Coastal Sciences Program

under contract number

N00014-84-C-0188

January 1985

ABSTRACT

This report consists of two parts. In Part I, a time dependent form of the reduced wave equation of Berkhoff is developed for the case of waves propagating over a bed consisting of ripples superimposed on an otherwise slowly varying mean depth which satisfies the mild slope assumption. The ripples are assumed to have wavelengths on the order of the surface wave length but amplitudes which scale as a small parameter along with the bottom slope. The theory is verified by showing that it reduces to the case of plane waves propagating over a one-dimensional, infinite patch of sinusoidal ripples, studied recently by Davies and Heathershaw and Mei. We then study two cases of interest; formulation and use of the coupled parabolic equations for propagation over patches of arbitrary form in order to study wave reflection, and propagation of trapped waves along an infinite ripple patch.

In the second part, we use the results of Part I to extend the results for weakly-nonlinear wave propagation to the case of partial reflection from bottoms with mild-sloping mean depth with superposed small amplitude undulations.

ACKNOWLEDGEMENT

This work was supported by the Office of Naval Research, Coastal Sciences Program under contract N00014-84-C-0188 through a contract with the University of Delaware. The author is grateful to Prof. R. A. Dalrymple for several conversations. The majority of the work in Chapter III was conducted while the author held a position at the Marine Sciences Research Center, State University of New York at Stony Brook. The technical assistance provided by the staffs of MSRC and COE is gratefully acknowledged, with a special thanks going to Cynthia J. Vey for typing the final report.

TABLE OF CONTENTS

LIST OF FIGURES

Chapter I

Summary

Wave models for waves propagating over uneven topography have undergone a great deal of development in the recent past, with the majority of work centered on the extreme examples of very abrupt topography, where the bottom may be reasonably schematized by sections of constant depth separated by discontinuities, and of topography with very mild bottom slopes, where the depth is assumed to change very slowly over the space of a wavelength. Although some of the work encompassed by the ongoing studies under the present ONR support have dealt with the first example (Kirby and Dalrymple, 1983a, plus continuing work on trenches and dredged channels with currents), most of the effort in the present contract period has dealt with the mild-slope extreme, where the basic formulations are either in the form of reduced wave equations (Berkhoff, 1972; Kirby, 1984) or WKB formulations giving evolution equations for the slowly varying domain (Chu and Mei, 1970; Djordjevic and Redekopp, 1978).

This report presents two theoretical results which extend the capabilities for modelling waves in shallow water. Chapter II presents a linear, reduced wave equation which is applicable to the case of waves propagating over bottom undulations which are small in amplitude but which may have length scales on the order of the surface wavelength. This formulation extends the basic mild-slope equation to the case of abrupt bars or similar topography resting on an otherwise mildly sloping bottom. Comparisons to previous theoretical and experimental results are given.

In Chapter III, the results of Chapter II are combined together with the coupled forward- and backward-scattered wave formulation of Liu and Tsay

(1983) and the perturbation method based on a Lagrangian formulation (Kirby, 1983) in order to develop a model for the gradual reflection of weakly nonlinear Stokes waves. Numerical results are given for several examples involving waves propagating in one and two dimensions.

Chapter II

A General Wave Equation for Waves over Rippled Beds

.1 Introduction

The problem of reflection of surface waves by patches of large bottom dulations has received an increasing amount of attention recently, due to is mechanism's possible importance in the development of shore-parallel rs. Davies and Heathershaw (1984) and Mei (1984) have recently studied the se of reflection from sinusoidal topography and have provided analytic eatments which elucidate the mechanism of a resonant Bragg reflection at the int where the wavelength of the bottom undulation is one half the wavelength the surface wave. The analytic results of both studies are seen to agree ite well with the laboratory data of Davies and Heathershaw (1984, riginally presented by Heathershaw, 1982). Based on the analytic and xperimental results, Mei suggests that reflection of waves from an initially solated bar (such as a break-point bar formed at the outer edge of the urfzone) may be sufficient to induce the formation of bars further offshore f the initial bar.

The analytic results presented to date illustrate the major features to e expected when studying reflection from a system of bars. However, they are oo limited in scope to provide a direct treatment in the case of natural bed orms varying arbitrarily in two horizontal directions. For this reason, the resent study concentrates on the development of a general wave equation which s applicable to linear surface waves in intermediate or shallow water epths. The resulting equation is similar in spirit to the reduced wave quation of Berkhoff (1972), but extends the usual mild-slope approximation to nclude rapidly-varying, small-amplitude deviations from the slowly-varying ean depth.

After deriving the general equation in Section 2, we consider the correspondence between the present results and those of Mei (1984) in Section 3. A simple numerical scheme is then used to solve the reduced wave equation for the case of reflection over one-dimensional topographies.

In Section 4, we apply a splitting method in order to reduce the elliptic form to two coupled parabolic equations for forward and backscattered waves. The resulting equations for amplitude of the forward and backward propagating waves extend the results of Mei to the case of arbitrary topographic variations and include possible diffraction effects.

Finally, in Section 5 we consider the possibly interesting case of trapped waves propagating along a ripple patch. The problem is developed as an eigenvalue problem for the wavelength along the patch, which is then solved numerically for the case of arbitrary topography, following the method of Kirby, Dalrymple and Liu (1981).

II.2 Derivation of the Wave Equation

The depth-integrated wave equation for monochromatic, linear waves propagating over small-amplitude bed undulations may be formulated following either a variant of the Green's formula method of Smith and Sprinks (1975) or Liu (1983), or by using the Lagrangian formulation of Kirby (1984). Here the Green's formula approach is utilized; indications of how to proceed in the Lagrangian approach are included at the end of the section.

Let $h'(\underset{\sim}{x})$, $\underset{\sim}{x} = \{x,y\}$ denote the total still water depth, and let

$$h' = h(\underset{\sim}{x}) - \delta(\underset{\sim}{x}) \tag{2.1}$$

where $h(\underset{\sim}{x})$ is a slowly varying depth satisfying the mild-slope assumption.

Unfortunately, no laboratory data exists to test these hypotheses; rification of the present results and conjectures thus require further dependent effort.

.4 Coupled Parabolic Equations for Forward and Back-scattered Waves

We now consider the development of coupled parabolic equations for rward and back-scattered waves, following the results of Radder (1979) and u and Tsay (1983). The goal is to obtain an extension to the refraction sults of Mei (1984) (as in 3.5 and 3.6) to cover cases where δ varies bitrarily in x and y, and where y-variations in δ or h may induce fficiently strong amplitude variations to warrant the introduction of ffraction effects. We take x to correspond to a principal propagation rection and assume that deviations from this direction are small. eglecting time dependence in the wave amplitude, (2.11) may be written in lliptic form as

$$p\hat{\phi}_{xx} + p_x\hat{\phi}_x + k^2 CC_g\hat{\phi} + (CC_g\hat{\phi}_y)_y - \frac{4\omega\Omega'}{k}(\delta\hat{\phi}_y)_y = 0 \qquad (4.1)$$

ere

$$p = CC_g - \frac{4\omega\Omega'\delta}{k} \qquad (4.2)$$

d where

$$p_x = (CC_g)_x - \frac{4\omega\Omega'}{k}\delta_x + O(k\delta)^2 \ . \qquad (4.3)$$

4.1) may be written as

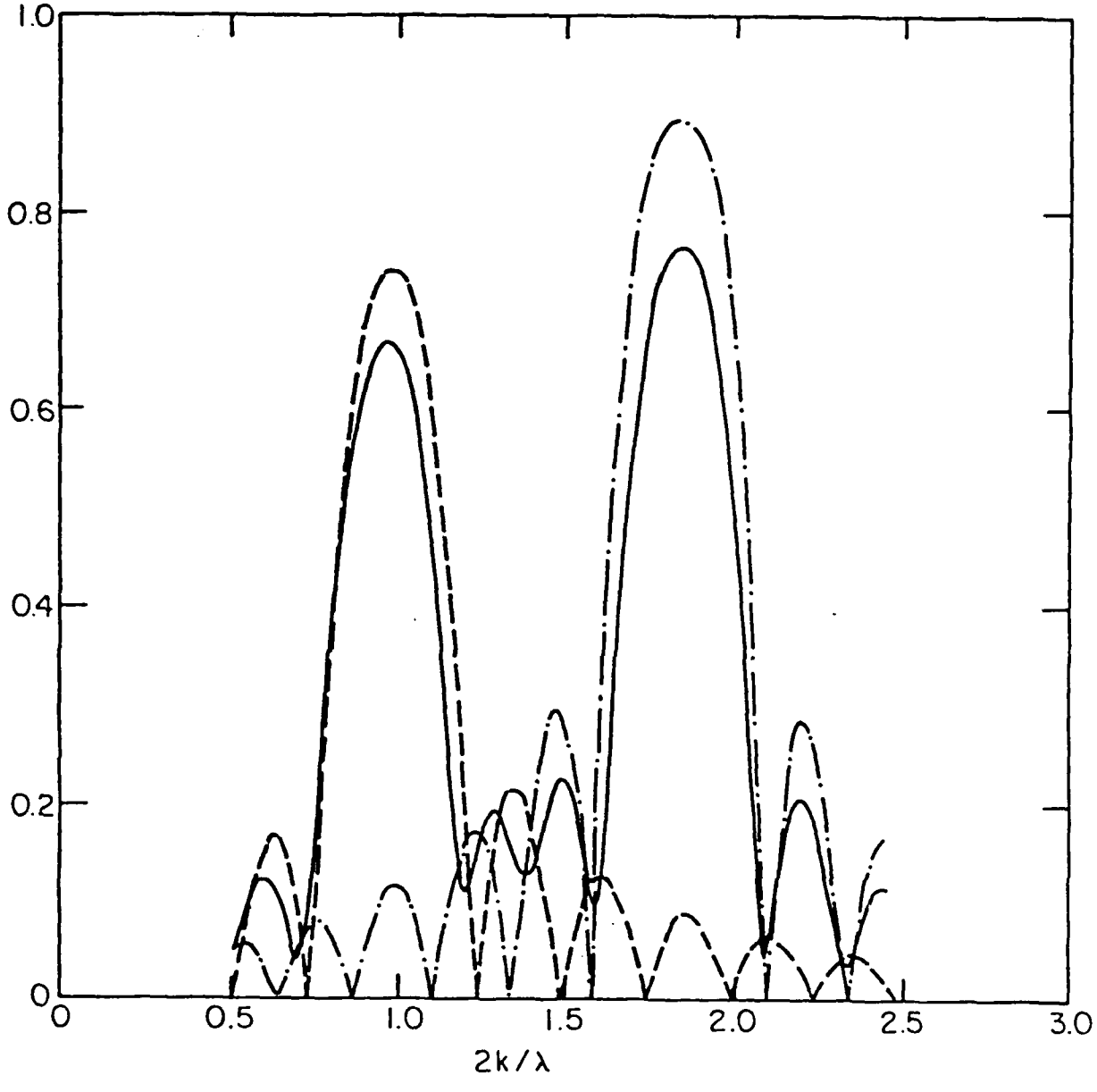

Figure II.5. Reflection from a patch with two Fourier components, $\delta = D_1 \sin\lambda_x + D_2 \sin(15\lambda x/8)$, n=4. ---, $D_1/h = 0.32$, $D_2/h = 0.0$; ——, $D_1/h = 0.0$, $D_2/h = 0.32$; ——, $D_1/h = D_2/h = 0.226$.

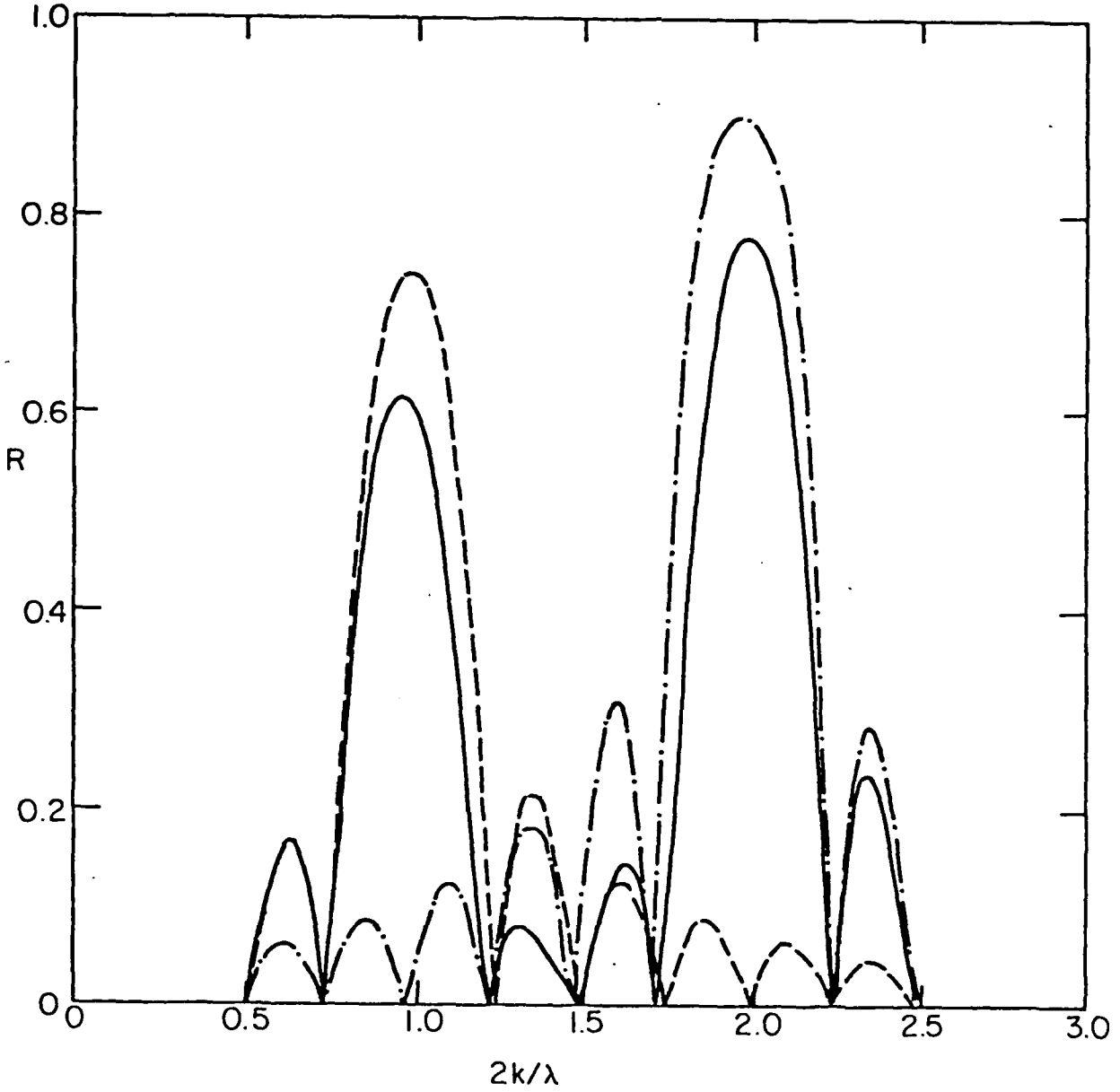

Figure II.4. Reflection from a patch with two Fourier components, $\delta = D_1 \sin\lambda x + D_2 \sin 2\lambda x$, $n = 4$. --- $D_1/h = 0.32$, $D_2/h = 0.$; ——— $D_1/h = 0.$, $D_2/h = 0.32$; ——— $D_1/h = D_2/h = 0.226$.

For case one, we use the data of Figure II.3 and set m=2 so that the second wave has half the wavelength of the first. Three situations are plotted in Figure II.4; $D_1/h = 0.32$, $D_2/h = 0.0$ (as in Figure II.3); $D_1/h = 0.0$, $D_2/h = 0.32$ (all variance at the shorter wavelength); and $D_1/h = D_2/h = 0.226$ (variance evenly divided between each component). The composite bottom is seen to produce the same zeroes in R, and a peak in R associated with resonance with each component of the bottom is apparent. The two resonance peaks remain separate and clearly distinguishable.

For the second case, we use n=4 and m=15/8, so that the second component has 7 1/2 wavelengths in the ripple patch. Curves of R for the same three distributions of ripple amplitudes as described above are given in Figure II.5. Now the reflection coefficients associated with each component acting separately have different zeroes. The two patterns together interact and destroy the zeroes; the resulting curve of R varies smoothly over the range of $2k/\ell$ considered. The peaks associated with resonant scattering from each component are again distinct and strong.

The strength of resonant reflection from an organized barfield implies that a broad spectrum containing a band of wavelengths which are nearly or exactly resonant with the bottom may experience fairly significant reduction in energy density near the resonance wave number. Further, the reflected wave field, which may assume the form of a fairly narrow spectral band around the resonant wave number, may be much "groupier" than the incident wave field. This groupiness may lead to significant forced long wave motions propagating in the offshore direction. These motions would be similar in form to the offshore propagating long wave caused by wave-group pumping of the surf zone (studied recently by Symonds and Bowen, 1984, and Symonds, Huntley and Bowen, 1982), but do not require the incident wave field to be distinctly groupy in nature.

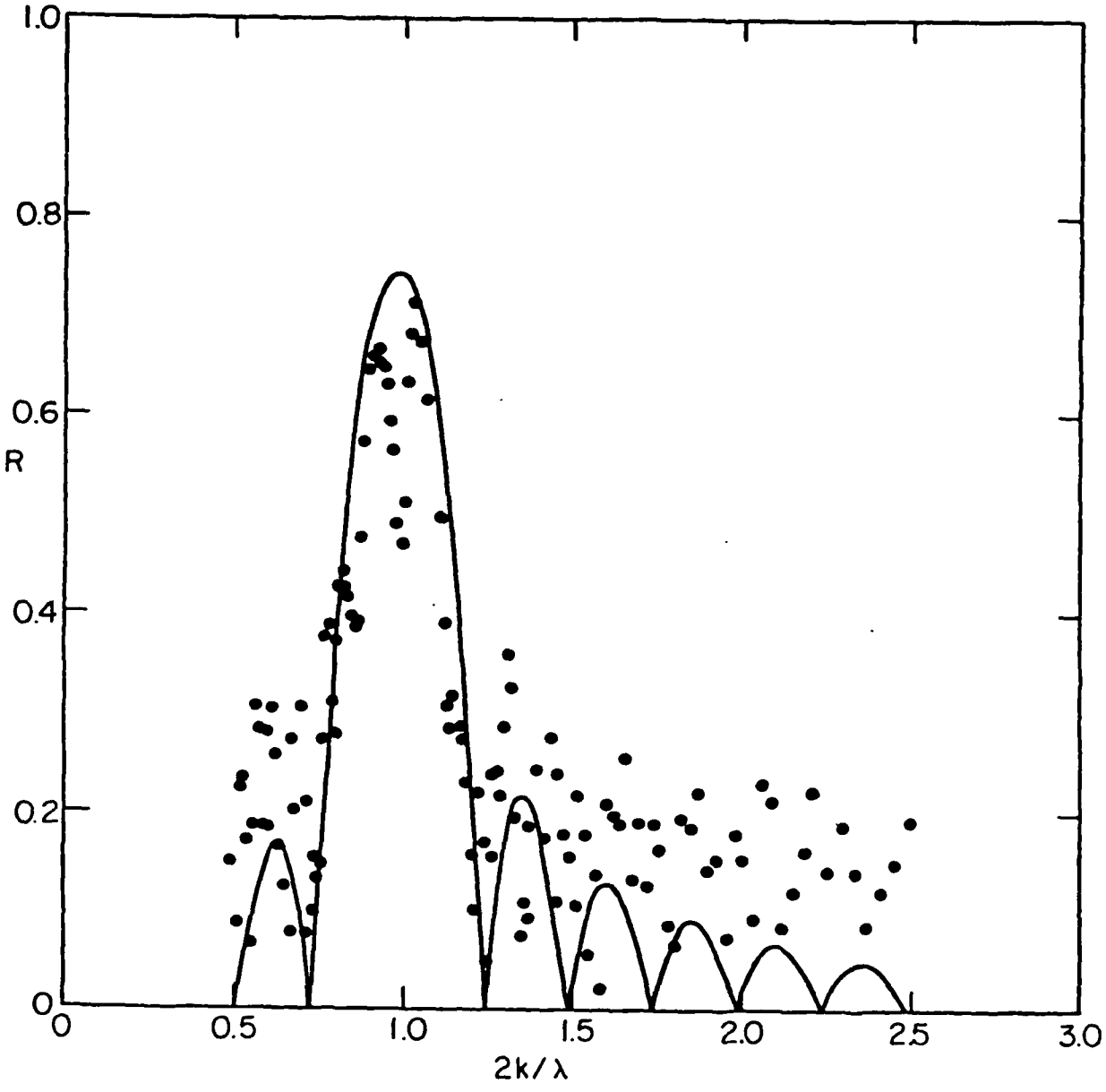

Figure II.3. Reflection coefficient for waves normall· incident on a sinusoidal patch. Case 2: D/h = 0.32, n = 4. —— numerical results; ● laboratory data from Davies and Heathershaw (1984)

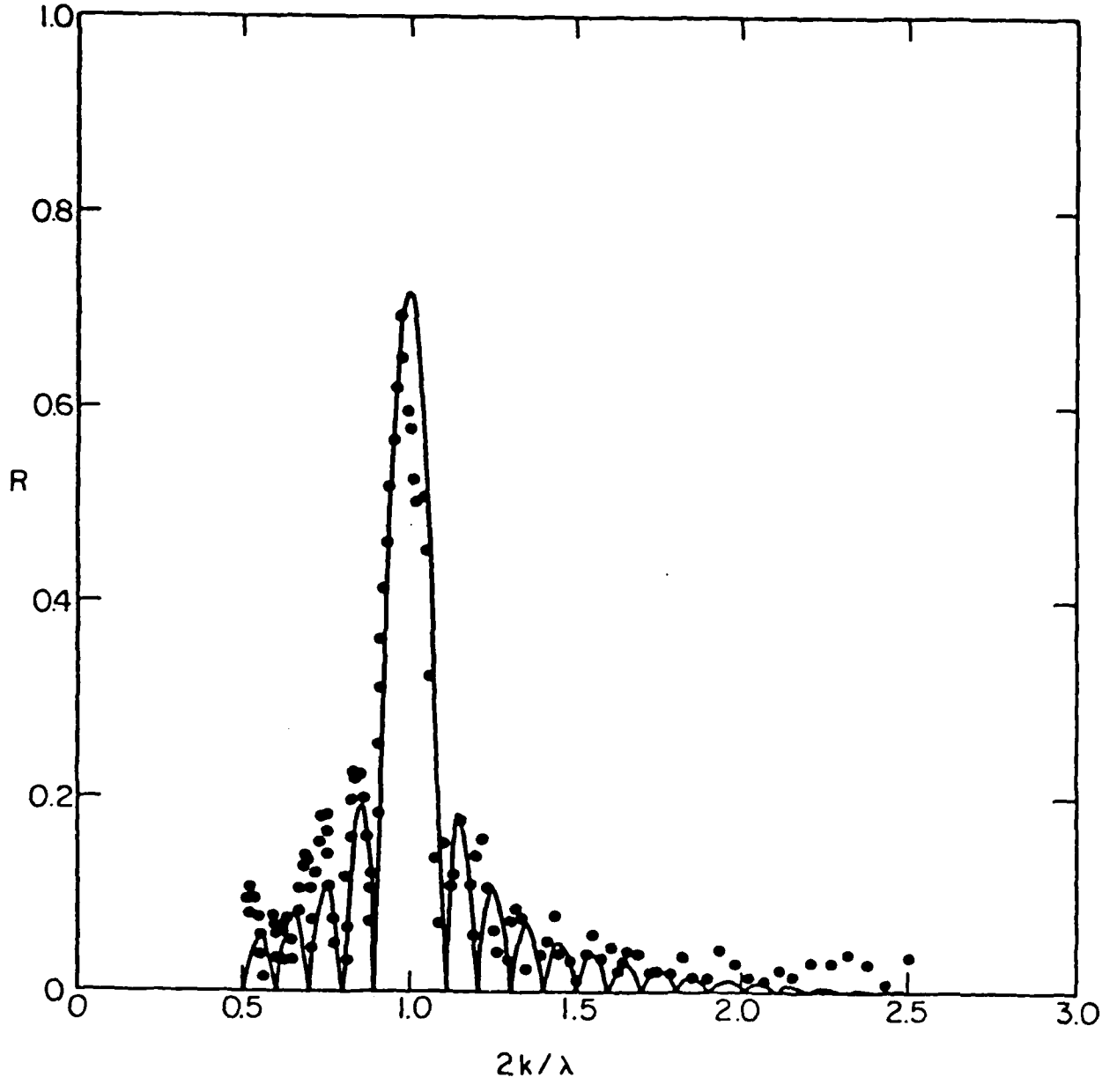

Figure II.2. Reflection coefficient for waves normally incident on a sinusoidal patch. Case 1: D/h = 0.16, n = 10. —— numerical results; ● laboratory data from Davies and Heathershaw (1984)

are given in Figures II.2 and II.3 for cases 1 and 2, respectively in comparison to the laboratory data. Solutions were obtained using a grid spacing of $\Delta x = \ell/20$ in order to obtain accurate results at large $2k/\lambda$. The numerical results are nearly indistinguishable from the analytic results of Davies and Heathershaw (1984) with the exception of an occasional downshift in the positions of the peaks and zeroes of R by an amount $2k/\lambda \sim 0.01$. This shift may be due to the neglect of nonpropagating waves at the ripple patch edges as well as the numerical errors involved in the computation scheme. The results are based on the same information as in Mei's approach, and compare well to his predictions over the range of validity of the theory for near-resonance.

Laboratory data from Davies and Heathershaw are included in Figures II.2 and II.3 for comparison to the numerical results. Davies and Heathershaw provide indications of how much the data at low R is contaminated by reflections at the end of the wave channel; no effort has been made to correct the data for this effect.

As a second example, we consider the reflection of waves from a bed formed by the superposition of two Fourier components.

$$\delta = D_1 \sin\lambda x + D_2 \sin m\lambda x \qquad 0 \leq x \leq 2\pi n/\lambda$$

We consider two cases; one where both Fourier components have an integral number of wavelengths in the ripple patch, and the other where the ripple patch terminates at a half wavelength for the second component. These cases differ since, for case one, the zeroes of the reflection coefficient for each component separately coincide; while for the second case the zeroes for each component do not coincide.

$$\delta = D\sin(\lambda x) \qquad 0 \leq x \leq n\ell \tag{3.11}$$

where $\ell = 2\pi/\lambda$ is the bed wavelength and n is the number of bed ripples. The Bragg-scattering condition corresponds to $2k/\lambda = 1$. Equation (3.8) is written in finite difference form, and radiating boundary conditions are applied according to

$$\hat{\phi}_x = -ik(\hat{\phi} - 2\hat{\phi}_I) \quad x_1 < 0 \tag{3.12}$$

$$\hat{\phi}_x = ik\hat{\phi} \qquad x_2 > n\ell \tag{3.13}$$

where

$$\hat{\phi}_I = e^{ikx} \tag{3.14}$$

is the incident wave of unit amplitude. The resulting tridiagonal matrix is inverted using a double-sweep algorithm.

We first consider the experimental results of Davies and Heathershaw and compare numerical results to the cases

1. $n = 10$, $D/h = 0.16$
2. $n = 4$, $D/h = 0.32$

Computed results for reflection coefficient R corresponding to a reflected wave

$$\phi_R = Re^{-ikx} \quad ; \quad x < 0 \tag{3.15}$$

Mei. All of Mei's subsequent results may be obtained from (2.11) following this procedure and his assumptions.

For later use, we define an unscaled frequency-like term Ω' according to

$$\Omega_o = \Omega'(kD) \tag{3.7}$$

where $\Omega' \sim 0\ (1)$. Ω' will be advantageous in the general case since it is not dependent on the geometry of the undulations. (Note that Ω' may still be a slowly varying function of the mean depth.)

II.3.2 One-Dimensional Reflection from a Ripple Patch

We now test the reduced, elliptic form of (2.11) for the case of waves normally incident on a finite ripple patch. Variations in the y-direction are neglected; the resulting problem is equivalent to that studied by Davies and Heathershaw if we restrict attention to sinusoidal undulations of constant amplitude and constant mean depth h. After setting h = constant, (2.11) reduces to

$$\hat{\phi}_{xx} + k^2\hat{\phi} - 4\left(\frac{\Omega'}{C_g}\right)(\delta\phi_x)_x = 0 \tag{3.8}$$

where

$$\tilde{\phi} = \hat{\phi}(x)\ e^{-i\omega t}\ , \tag{3.9}$$

Ω' is defined by

$$\Omega' = \frac{gk}{4\omega\ \cosh^2 kh} \tag{3.10}$$

following (3.7), and where we have neglected time dependence in the wave amplitude. For the case of sinusoidal bed oscillations, we may take

We consider an incident wave

$$\tilde{\phi}^{+} = -\frac{ig}{2\omega} A(x,t)\, e^{i(kx-\omega t)} \tag{3.1}$$

and reflected wave

$$\tilde{\phi}^{-} = -\frac{ig}{2\omega} B(x,t)\, e^{i(-kx-\omega t)} \tag{3.2}$$

where A and B are slowly varying functions of x and t. The conditions for resonant Bragg- scattering are satisfied when the bottom undulation has a wavelength of one-half the surface wavelength, or

$$\lambda = 2k \tag{3.3}$$

Employing this assumption, we proceed by assuming that derivatives of A and B are $O(k\delta)$ in comparison to A and B and keep terms only to $O(k\delta)$. Defining

$$\Omega_o = \frac{gk^2 D}{4\omega \cosh^2 kh} \tag{3.4}$$

and collecting terms of like powers in e^{ikx}, we obtain

$$A_t + C_g A_x = -i\Omega_o B \tag{3.5}$$

$$B_t - C_g B_x = -i\Omega_o A \tag{3.6}$$

which is a special case of the results of Mei, neglecting mean bottom slope and oblique angle of incidence. Solutions of (3.5) and (3.6) in relation to the experimental results of Davies and Heathershaw are discussed in detail by

$$L = \int_{-h'}^{\eta} \left\{ \phi_t + \frac{1}{2} (\nabla_h \phi)^2 + \frac{1}{2} (\phi_z)^2 + gz \right\} dz$$

and then expanding the integral about $z = -h$. Equations (2.10) and (2.11) follow after collecting terms of $O(ka)^2$ and partially integrating the variation of the integral of L over the propagation space, as in Kirby (1984).

II.3 Correspondence to Previous Results

In order to demonstrate the completeness and generality of the wave equation (2.11), we first consider a reduction of the equation to the coupled evolution equations of Mei (1984) for resonant Bragg-scattering by a finite patch of ripples. We then employ a finite difference form of (2.11), after neglecting time dependence, to study the one-dimensional (x only) reflection for a range of incident wavelengths, and compare our results to the data presented by Davies and Heathershaw (1984).

II.3.1 Resonant Bragg-scattering

Consider the particular example, studied by Davies and Heathershaw (1984) and Mei (1984), of waves propagating normally over a ripple patch extending uniformly to $\pm \infty$ in y. Depth h is taken to be constant, while δ is given by

$$\delta = \frac{D}{2} (e^{i\lambda x} + e^{-i\lambda x}) \quad ; \quad 0 \leq x \leq L \ ,$$

where $0 \leq x \leq L$ is the range of the ripple patch, and

$$\delta = 0 \quad ; \quad x < 0 \ , \quad x > L$$

$$\int_{-h}^{0} f\phi_{zz}\,dz - \int_{-h}^{0} \phi\, f_{zz}\,dz = \left[f\phi_z - \phi f_z\right]_{-h}^{0} \tag{2.9}$$

The integrals are manipulated to finally obtain

$$\tilde{\phi}_{tt} - \nabla_h\cdot(CC_g\nabla_h\tilde{\phi}) + (\omega^2 - k^2CC_g\tilde{\phi}) + gf^2 \Big|_{-h} \nabla_h\cdot(\delta\nabla_h\tilde{\phi})$$

$$+ g\int_{-h}^{0} f\nabla_h^2 f\, dz\tilde{\phi} + gf\nabla_h f\cdot\nabla_h h \Big|_{-h} \tilde{\phi}$$

$$+ gf\nabla_h f\cdot\nabla_h\delta \Big|_{-h} \tilde{\phi} + g\delta(f\nabla_h^2 f) \Big|_{-h} \tilde{\phi}$$

$$+ 2g\delta f\nabla_h f\cdot\nabla_h\tilde{\phi} \Big|_{-h} = 0 \tag{2.10}$$

where $C = \omega/k$ and $C_g = \partial\omega/\partial k$. The last five terms are either proportional to $(\nabla_h h)^2$ or $\delta\nabla_h h$, and are thus second order in the small parameter. Neglecting them and substituting for $f(z = -h)$ then gives

$$\tilde{\phi}_{tt} - \nabla_h\cdot(CC_g\nabla_h\tilde{\phi}) + (\omega^2 - k^2CC_g)\tilde{\phi} + \frac{g}{\cosh^2 kh}\nabla_h\cdot(\delta\nabla_h\tilde{\phi})$$

$$= O(k\delta)^2 \tag{2.11}$$

Equation (2.11) governs the value of the potential at the free surface for an arbitrary wave motion. Neglecting the term in δ yields a time dependent form of Berkhoff's (1972) equation for the slowly varying bottom alone.

This completes the derivation using the Green's identity method. The Lagrangian formulation proceeds by writing the integral of the total pressure over the local depth

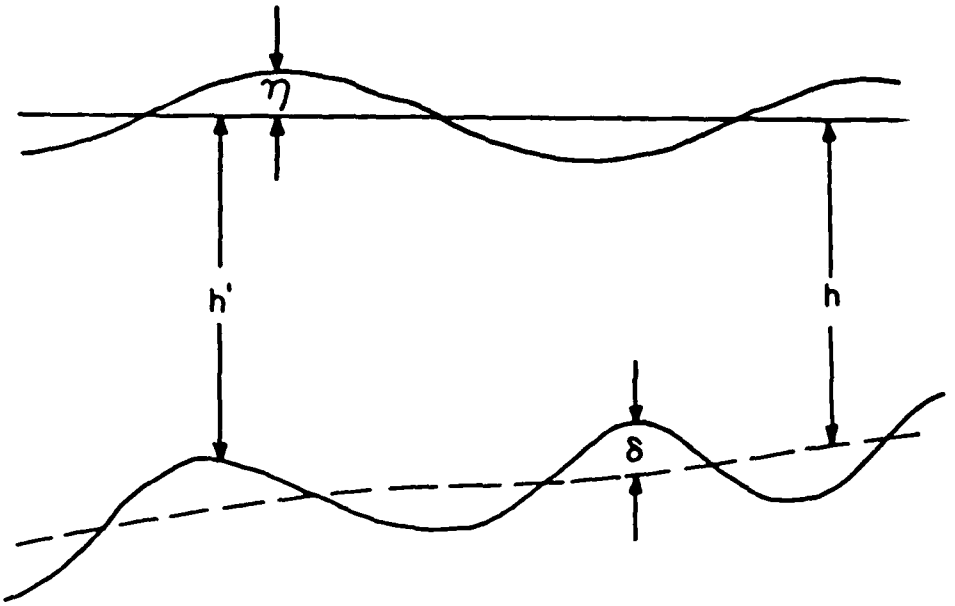

Figure II.1. Definition of depth components

$$\nabla_h h/kh \ll 1 \quad , \quad \nabla_h = (\partial/\partial x \ , \ \partial/\partial y) \tag{2.2}$$

$\delta(\underset{\sim}{x})$ represents rapid undulations of the depth about the mean level, as indicated in Figure II.1. We consider the problem to be linearized in wave amplitude but retain first order terms in the bed undulation amplitude. We assume

$$O(\nabla_h h/kh) \sim O(k\delta) \ll 1 \tag{2.3}$$

Linearizing the free surface boundary conditions and expanding the bottom boundary condition about $z = -h$, we obtain to $O(k\delta)$

$$\nabla_h^2 \phi + \phi_{zz} = 0 \ ; \ -h \leq z \leq 0 \tag{2.4}$$

$$\phi_{tt} + g\phi_z = 0 \ ; \ z = 0 \tag{2.5}$$

$$\phi_z = -\nabla_h h \cdot \nabla_h \phi + \nabla_h \cdot (\delta \nabla_h \phi) \ ; \ z = -h \tag{2.6}$$

To leading order, the solution to (2.4) - (2.6) may be expressed as

$$\phi(\underset{\sim}{x},z,t) = f(\underset{\sim}{x},z)\ \tilde{\phi}(\underset{\sim}{x},t) + \Sigma \text{ non-propagating modes} \tag{2.7}$$

where $f = \cosh k(h+z)/\cosh kh$ is a slowly varying function of $\underset{\sim}{x}$, and where

$$\omega^2 = gk \tanh kh \tag{2.8}$$

locally, with ω being the fixed angular frequency and k the wavenumber. We then use Green's second identity to extract the propagating component of ϕ;

$$\hat{\phi}_{xx} + p^{-1}p_x\hat{\phi}_x + k^2CC_gp^{-1}\hat{\phi} + p^{-1}(CC_g\hat{\phi}_y)_y - \frac{4\omega\Omega' p^{-1}}{k}(\delta\phi_y)_y \qquad (4.4)$$

where, to leading order in $(k\delta)$, p^{-1} is given by

$$p^{-1} = (CC_g)^{-1}\left\{1 + 4\left(\frac{\Omega'}{C_g}\right)\delta + O(k\delta)^2\right\} \qquad (4.5)$$

Next we denote an operator $\gamma^2\phi$ according to

$$\gamma^2\phi = k^2CC_gp^{-1}\phi + p^{-1}(CC_g\phi_y)_y - \frac{4\omega\Omega' p^{-1}}{k}(\delta\phi_y)_y$$

or

$$\gamma^2\phi = k^2\left\{\left(1 + 4\left(\frac{\Omega'}{C_g}\right)\delta\right)\phi + \frac{1}{k^2CC_g}(CC_g\phi_y)_y - \frac{4}{k^2}\left(\frac{\Omega'}{C_g}\right)(\delta\phi_y)_y\right\}$$

$$+ O(k\delta)^2 \qquad (4.6)$$

The corresponding pseudo-operator $\gamma\phi$ is obtained by the expanding the square root to give

$$\gamma\phi = k\left\{\left(1 + 2\left(\frac{\Omega'}{C_g}\right)\delta\right)\phi + \frac{1}{2k^2CC_g}(CC_g\phi_y)_y - \frac{2}{k^2}\left(\frac{\Omega'}{C_g}\right)(\delta\phi_y)_y\right\}$$

$$+ O(k\delta)^2 \qquad (4.7)$$

We now follow a simple scheme for obtaining the coupled parabolic equations. Let $\hat{\phi}$ be expressed as the sum of forward and backward propagating waves;

$$\hat{\phi} = \phi^+ + \phi^- \qquad (4.8)$$

We then assume the coupled equations:

$$\phi_x^+ = i\gamma\phi^+ + F(\phi^+,\phi^-)$$

$$\phi_x^- = -i\gamma\phi^- - F(\phi^+,\phi^-) \qquad (4.9)$$

where the coupling term F is unknown. Repeated substitution of (4.9) in (4.4) finally yields

$$F(\phi^+,\phi^-) = -\frac{(\gamma p)_x}{2\gamma p}(\phi^+ - \phi^-) \qquad (4.10)$$

which may be expanded to give

$$F(\phi^+,\phi^-) = -\left\{\frac{(kCC_g)_x}{2kCC_g} - \left(\frac{\Omega'}{C_g}\right)\delta_x\right\}(\phi^+ - \phi^-) \qquad (4.11)$$

to leading order in $(k\delta)$. The coupled equations in expanded form are given by

$$\phi_x^+ = ik\left\{1 + 2\left(\frac{\Omega'}{C_g}\right)\delta\right\}\phi^+ + \frac{i}{2kCC_g}(CC_g\phi_y^+)_y$$

$$- \frac{2i}{k}\left(\frac{\Omega'}{C_g}\right)(\delta\phi_y^+)_y - \frac{(kCC_g)_x}{2kCC_g}(\phi^+ - \phi^-)$$

$$+ \left(\frac{\Omega'}{C_g}\right)\delta_x(\phi^+ - \phi^-) \quad ; \qquad (4.12)$$

$$\phi_x^- = -ik\left\{1 + 2\left(\frac{\Omega'}{C_g}\right)\delta\right\}\phi^- - \frac{i}{2kCC_g}(CC_g\phi_y^-)_y$$

$$+ \frac{2i}{k}\left(\frac{\Omega'}{C_g}\right)(\delta\phi_y^-)_y + \frac{(kCC_g)_x}{2kCC_g}(\phi^+ - \phi^-)$$

$$- \left(\frac{\Omega'}{C_g}\right)\delta_x(\phi^+ - \phi^-) \; . \qquad (4.13)$$

We introduce the complex amplitudes A,B according to

$$\phi^{+} = -\frac{ig}{\omega} A e^{ik_o x}$$

$$\phi^{-} = -\frac{ig}{\omega} B e^{-ik_o x}$$

where k_o is a reference wavenumber. (4.12) and (4.13) become

$$2ikCC_g A_x + \{2k\,(k-k_o)\,CC_g + i(kCC_g)_x$$

$$+ 2\omega\Omega'\,[2k\delta - i\delta_x]\} A + (CC_g A_y)_y - \frac{4\omega\Omega'}{k}(\delta A_y)_y$$

$$= \{i(kCC_g)_x - 2i\omega\Omega'\delta_x\} B e^{-2ik_o x} \qquad (4.14)$$

$$2ikCC_g B_x + \{-2k(k-k_o)\,CC_g + i(kCC_g)_x$$

$$-2\omega\Omega'\,[2k\delta + i\delta_x]\} B - (CC_g B_y)_y + \frac{4\omega\Omega'}{k}(\delta B_y)_y$$

$$= \{i(kCC_g)_x - 2i\omega\Omega'\delta_x\} A e^{2ik_o x} \qquad (4.15)$$

The correspondence between the present equations and the results in Section 3.1 may be seen by substituting for δ using (3.11) and neglecting terms with rapidly oscillating coefficients. Note that the equations developed by Mei neglect diffraction effects as well as the coupling between the forward and backward propagating waves over the slowly varying depth. The present equations include these effects. Further, they reduce to a set of equations equivalent to those of Liu and Tsay (1983) when δ is neglected.

In the following example, (4.14) - (4.15) are discretized according to the Crank-Nicolson method. The solution technique is equivalent to that used by Liu and Tsay; hence, the details are omitted here.

We construct a two-dimensional patch of ripples of finite extent in the x and y directions. Ripples with length ℓ are alligned with crests parallel to the y-axis. The patch is symmetric about the x-axis and has overall dimensions of $n\ell$ and $2n\ell$ in x and y, where n is the number of ripple wavelengths. The topography is given by h = constant and

$$\delta(x,y) = \begin{cases} D\sin(\lambda x)\cos(\lambda y/4n); \\ \qquad |x| \leq n\ell/2, \ |y| \leq n\ell \\ 0 \ ; \quad |x| > n\ell/2, \ |y| > n\ell \end{cases} \tag{4.16}$$

The computational domain is given by $-3 \leq x/\ell \leq 3$ and $0 \leq y/\ell \leq 6$. We consider ripples similar to those of Figure II.3, with D/h = 0.32 and n=4. Results were computed for the resonant case $2k/\lambda = 1$ and are plotted along with the bottom contours in Figures II.6a (for incident amplitude $|A|$) II.6b (for reflected amplitude $|B|$), and Figure II.6c (for the total wave field).

The present results were obtained using four iterations of the forward-backward calculation, which was sufficient to provide a reasonable degree of convergence. As in Section 3, a grid spacing of $\Delta x = \Delta y = \lambda/20$ was used. Unfortunately, no laboratory data exists to test the two-dimensional model; verification was limited to checking that results of the coupled parabolic model are equivalent to results using the elliptic model for the one-dimensional cases studied in Section 3.

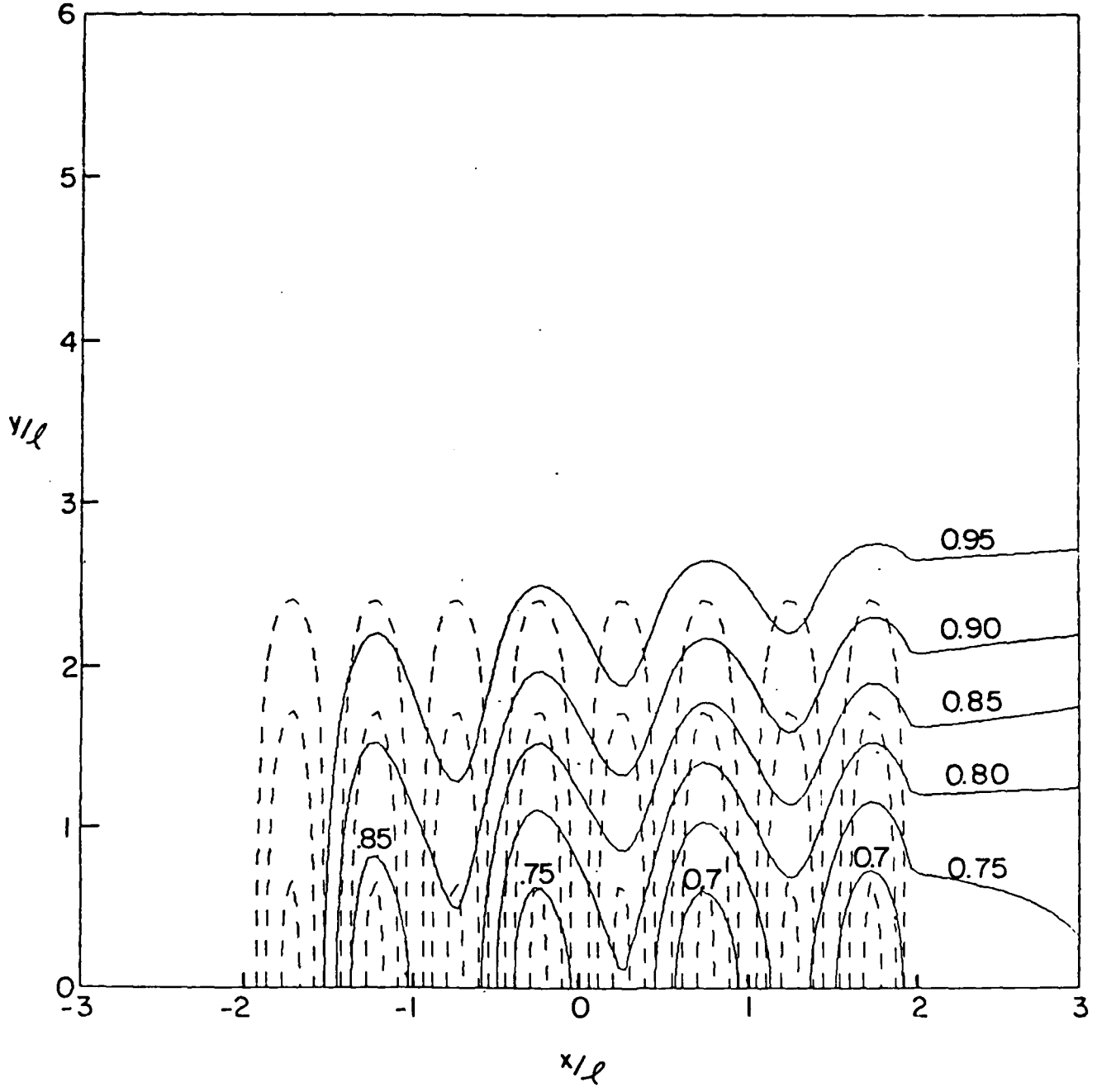

a) Incident wave field $|A/A_0|$

Figure II.6. Amplitude contours with respect to incident wave amplitude; waves propagating over two-dimensional ripple patch. — bottom contours; —— amplitude contours

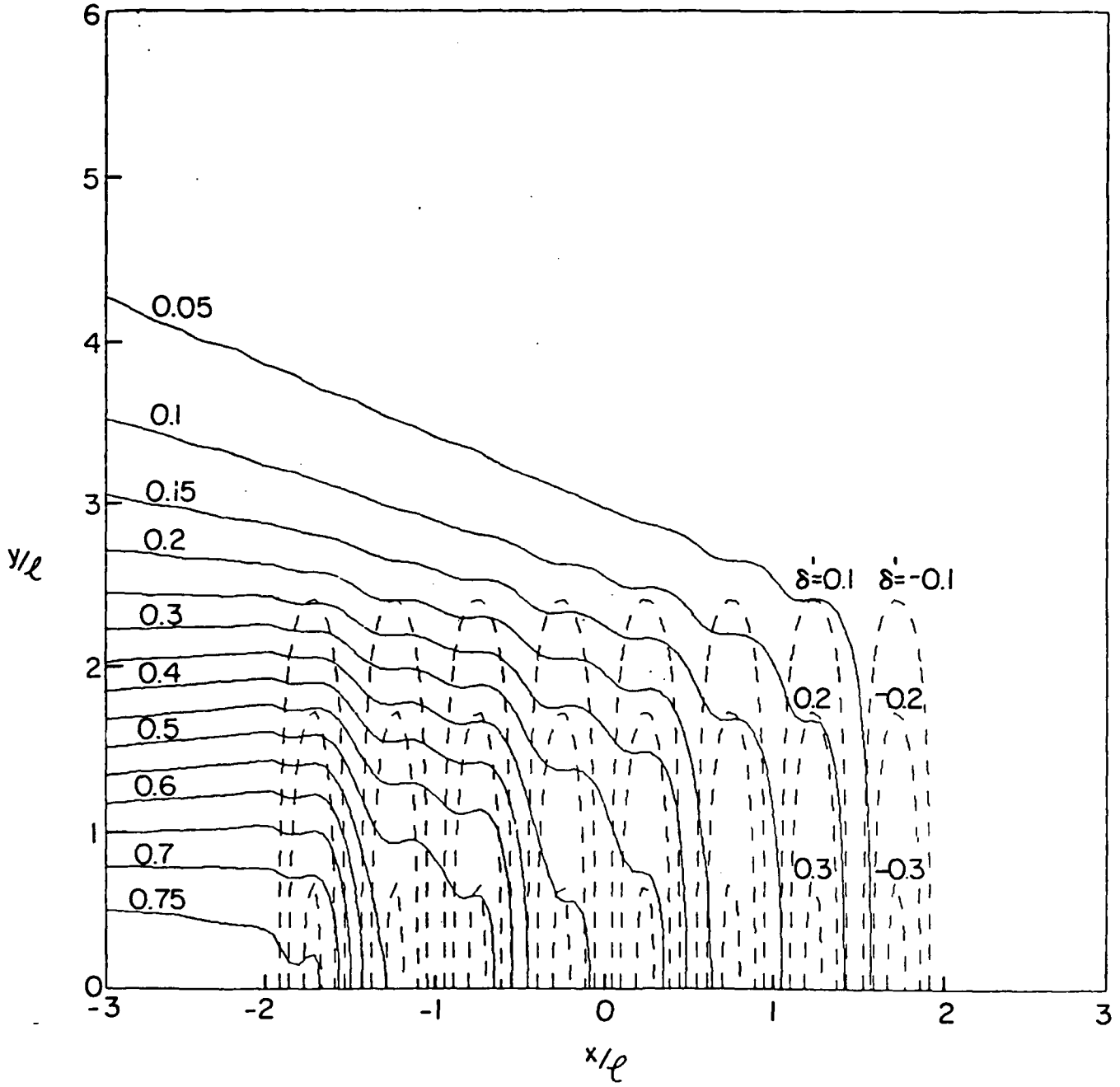

b) Reflected wave field $|B/A_o|$

Figure II.6. Continued

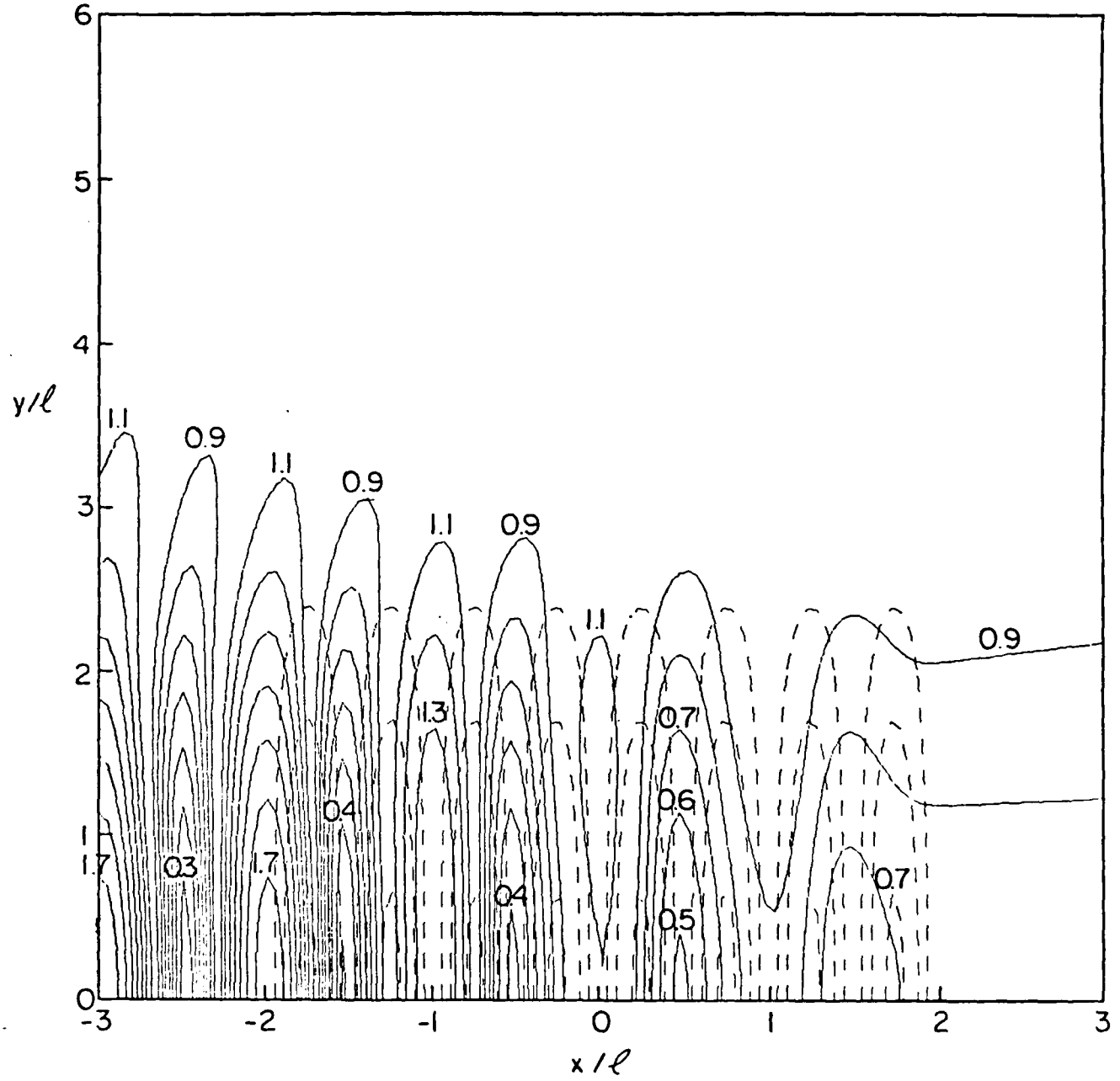

c) Total wave field

Figure II.6. Continued

II.5 Waves Trapped Over Long Ripple Patches

As a final example, we consider the propagation of a trapped wave along a ripple patch which extends to $y = \pm \infty$. This case has possible applications to the nearshore zone, where waves may be directed onto a nearshore bar system by reflection from headlands or coastal structures. This problem has been investigated previously in the context of the mild-slope approximation by Lozano (1977); the present analysis is presumably applicable to steeper bar systems than would be allowed for under the mild-slope assumption. Further, in the case of long coastally-trapped waves, the bar system may serve as a wave guide for trapped wave energy; Kirby et al (1981) have suggested that this trapping may effectively stabilize the offshore distribution of nodes and antinodes of infragravity edge waves, rendering the bar system less subject to destructive effects of a slowly changing wave climate.

The general case of trapped wave motion over a variety of offshore profiles may be handled in a manner similar to that provided by Kirby et al (1981); we remark that this method has also been used recently by McIver and Evans (1984) to study the waves trapped above a submerged horizontal cylinder located close to the water surface.

We denote ℓ as the longshore (y) component of the wave number vector and assume that h and δ are functions of x only (no longshore variation in the depth profile). Letting

$$\hat{\phi}(x,y) = \psi(x)e^{i\ell y}, \tag{5.1}$$

we obtain the second order ordinary differential equation governing $\psi(x)$;

$$\left\{CC_g - \frac{4\omega\Omega'\delta}{k}\right\}\psi_{xx} + \left\{(CC_g)_x - \frac{4\omega\Omega'\delta_x}{k}\right\}\psi_x$$

$$+ \left\{(k^2 - \ell^2)CC_g + \frac{4\omega\Omega'\ell^2\delta}{k}\right\}\psi = 0 \tag{5.2}$$

This then provides an eigenvalue problem for ψ and ℓ^2 which must be solved together with suitable boundary conditions. As a first example, we consider the simple case of a rectangular ridge of height D and width 2L resting on a flat bottom of depth h_1. The depth of water over the ridge is given by

$$h_2 = h_1 - D < h_1 \tag{5.3}$$

The geometry is shown in Figure II.7. This case is of interest because it may be solved analytically both by the present method as well as by using the mild slope equation in its basic form (see Smith and Sprinks, 1975, for the relevant formulation and matching conditions). In addition, the shallow water limits of both solutions may be compared to the results presented by Mei (1983, Section 4.6). This case then provides us with a means for evaluating the approximate upper limit on D/h_1, which is determined by checking for divergence of the solution for the present theory from the mild-slope theory as D/h_1 becomes large.

For the case of constant depth $h_2 = h_1 - D$ over the ridge and h_1 away from the ridge, we divide the fluid domain into three regions and obtain

$$\psi^{(2)}_{xx} + (k_1^2 - \ell^2)\,\psi^{(2)} = 0 \quad ; \quad x > L \tag{5.4a}$$

$$\psi^{(3)}_{xx} + (k_1^2 - \ell^2)\,\psi^{(3)} = 0 \quad ; \quad x < -L \tag{5.4b}$$

and

$$\alpha\psi^{(1)}_{xx} + (k_1^2 - \alpha\ell^2)\,\psi^{(1)} = 0 \quad ; \quad -L \leq x \leq L \tag{5.4c}$$

where k_1 is the wavenumber corresponding to h_1 and

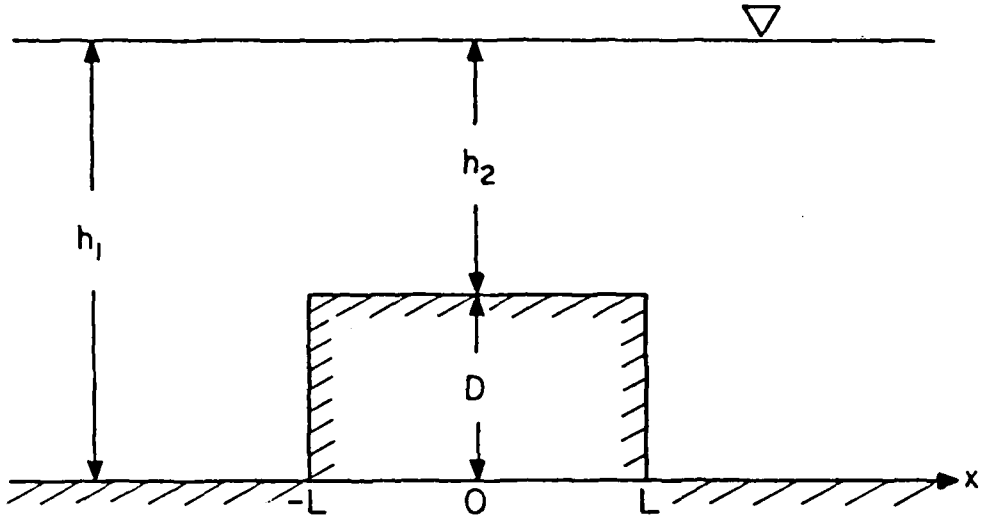

Figure II.7. Rectangular ridge for trapped wave example

$$\alpha = 1 - 4\left(\frac{\Omega'}{C_g}\right) D \tag{5.5a}$$

$$= 1 - \frac{2k_1 h_1}{n_1 \sinh 2k_1 h_1}\left(1 - \frac{h_2}{h_1}\right) . \tag{5.5b}$$

In order for trapped waves to exist, solutions must be exponentially decaying away from the ridge in regions 2 and 3. This requires that $\ell^2 > k_1^2$ while a separate condition on $\psi^{(1)}$ implies that $\ell^2 < k_1^2/\alpha$. The solutions for each region are given by

$$\psi^{(2)} = Ae^{-m(x-L)} \tag{5.6a}$$

$$\psi^{(3)} = Be^{m(x+L)} \tag{5.6b}$$

$$\psi^{(1)} = Ce^{i\lambda x} + De^{-i\lambda x} \tag{5.6c}$$

where A, B, C, D are arbitrary constants,

$$m = (\ell^2 - k_1^2)^{1/2} > 0 \quad , \tag{5.7}$$

and

$$\lambda = (k_1^2/\alpha - \ell^2)^{1/2} > 0 \tag{5.8}$$

Matching conditions are provided by considering the integral of the governing equation across the jump discontinuity at the ridge boundary; we get

$$\psi^{(1)} = \psi^{(2)} \qquad x = L \tag{5.9a}$$

$$\psi^{(1)} = \psi^{(3)} \qquad x = -L \tag{5.9b}$$

$$\alpha\psi_x^{(1)} = \psi_x^{(2)} \qquad x = L \tag{5.9c}$$

$$\alpha\psi_x^{(1)} = \psi_x^{(3)} \qquad x = -L \tag{5.9d}$$

The solution to (5.6 - 5.9) may be found in a straightforward manner; the notation of Mei (1983) is used to facilitate comparison to the shallow water case. Trapped waves are given by the solutions (for ξ) of the relation

$$\frac{\alpha\xi}{\left(\xi^{*2} - \xi^2\right)^{1/2}} = \begin{cases} \cot\xi & n \text{ even} \\ -\tan\xi & n \text{ odd} \end{cases} \tag{5.10}$$

where n is the mode number of the trapped wave. Here, ξ and ξ^* are given by

$$\xi = \left\{\left(k_1^2/\alpha - \ell^2\right)^{1/2}\right\} L = \lambda L \tag{5.11}$$

$$\xi^* = (k_1 L)\left((1 - \alpha)/\alpha\right)^{1/2} \tag{5.12}$$

The condition that $\xi < \xi^*$ from (5.10) provides an upper cutoff limit for n; n increases for increasing L or decreasing h_2 (increasing D).

Following Smith and Sprinks (1975), the mild-slope equation may be solved in analogous fashion. The solutions are given by (5.10) with the newly defined coefficients

$$\alpha = (CC_g)_2/(CC_g)_1 \tag{5.13a}$$

$$\lambda = (k_2^2 - \ell^2)^{1/2} \tag{5.13b}$$

$$\xi = \{(k_2^2 - \ell^2)^{1/2}\} L \tag{5.13c}$$

$$\xi^* = \{(k_2^2 - k_1^2)^{1/2}\} L \tag{5.13d}$$

or the case of the present geometry, where the mild-slope equation is valid xcept across the jump discontinuities, we may regard (5.10) together with 5.13) as a "correct" solution and compare those results to the present, small ottom amplitude solution given by (5.10) together with (5.8 - 5.12). omparing the various coefficients, we see that the present theory should pproximate the general depth, mild-slope theory well in regions where α from (5.5) is a good approximation to α from (5.13a), and where $k_1/\alpha^{1/2}$ (α from (5.5)) is fairly close to k_2.

Plots of the two α's and of the ratio $(k_1/\alpha^{1/2})/k_2$ are given in Figures II.8a and b for a range of h_2/h_1 and k_1h_1 values. Interestingly, the eviations between the two theories are greatest in the intermediate depth ange and apparently decrease in deepwater. This result is due to the fact hat the depth over the step becomes effectively deep unless h_2/h_1 is small, rendering the step ineffective in trapping or reflecting waves. In shallow ater, both theories give solutions which are asymptotic to the results given by Mei (1983). The asymptotic values of α and ξ^* are

$$\alpha = h_2/h_1$$

$$\xi^* = \left(\frac{\omega^2}{gh_2}\right)^{1/2} L\,(1 - h_2/h_1)^{1/2} \qquad h_1 \to 0 \tag{5.14}$$

The two theories are essentially different in intermediate depths; however, the results differ little over the range $0.6 < h_2/h_1 < 1.0$, or,

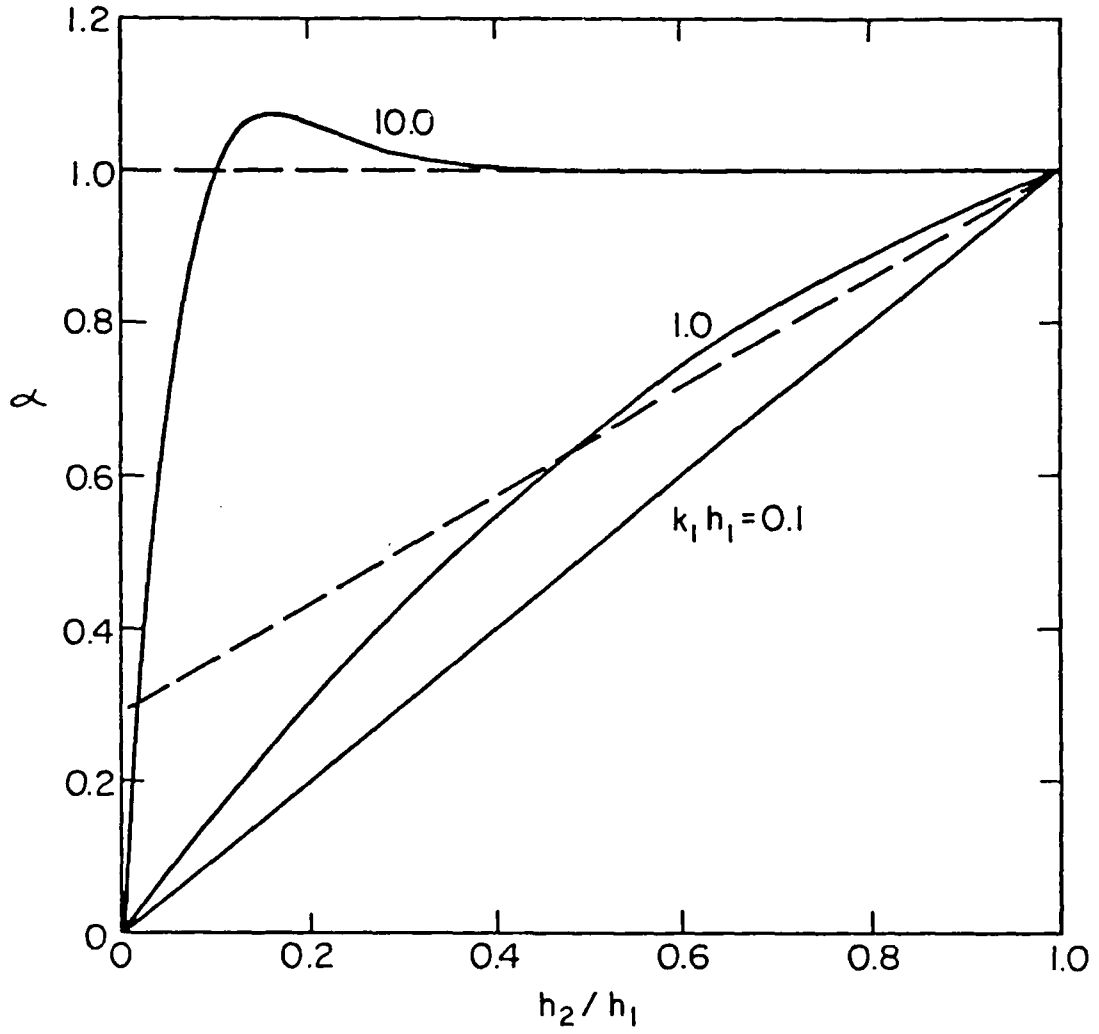

a) α; —— mild slope, --- small amplitude bottom theory

Figure II.8. Comparison of parameters for trapped waves over a rectangular ridge

$$+ b_2 = -\frac{\phi_2'}{g} - \frac{I_2''}{g}\tilde{\phi}_{2_t} + \frac{2I_1'''}{g^2}(\tilde{\phi}_{1_t})^2 - \frac{I_{1,1}''}{2g}(\nabla_h\tilde{\phi}_1)^2 - \frac{I^{z''}_{1,1}}{2g}\tilde{\phi}_1^2 \qquad (2.13)$$

ter eliminating η_1 according to (2.9). Variation of L_4 with respect
ϕ_2' and partial integration yields a continuity equation

$$(\eta_2 + b_2)_t + \nabla_h \cdot (h\nabla\phi_2') - \frac{1}{g}\nabla_h \cdot (\tilde{\phi}_{1_t}\nabla_h\tilde{\phi}_1) + \nabla_h \cdot (I_2'\nabla_h\tilde{\phi}_2) = 0 \qquad (2.14)$$

$\eta_2 + b_2$) may be eliminated between (2.13) and (2.14) to yield a forced wave
quation for the quasi-steady motion ϕ_2' after averaging over the phase.

The equation containing the nonlinear modification to the linear wave
quation (2.11) may be obtained by varying $L_2 + L_4$ together by η_1 and $\tilde{\phi}_1$ and
liminating η_1, yielding

$$\varepsilon\{\tilde{\phi}_{1_{tt}} - \nabla_h\cdot(CC_g\nabla_h\tilde{\phi}_1) + (\omega^2 - k^2CC_g)\tilde{\phi}_1\} = \varepsilon^3\{\text{N.L.T.}\} \qquad (2.15)$$

N.L.T.} is a complicated expression involving products of $\tilde{\phi}_1$, $(\eta_2 + b_2)$,
$_2$ and ϕ_2', and is given in Appendix III.C for completeness. We remark that
erms in {N.L.T.} have been manipulated by substitution using the linearized
elationships, in analogous form to the treatment of higher order terms in the
oussinesq wave formulation. Equation (2.15) is in the form of a second order
yperbolic equation for a general wave motion in {x,y,t}; however, {N.L.T.}
ontains components proportional to the third harmonic $\tilde{\phi}_3$. These terms are
liminated in the derivation of the evolution equations. An equation similar
o (2.15) has been given previously by Liu and Tsay (1984) for the case of
rogressive waves.

at parameter, it is clear that the linear equation governing the behavior of parameter of $O(\varepsilon^n)$ will come from the variation of L_{2n} with respect to that rameter. Thus the linear equation governing $\tilde{\phi}_1$ will be contributed by L_2, ile L_4 will contribute the $O(\varepsilon^3)$ terms in phase with $\tilde{\phi}_1$.

We now derive governing equations which are generally applicable to any otion described by the potential (2.4a) L_0 and L_1 contribute nothing in this pproximation. The linear wave equation is derived by first varying L_2 with espect to η_1, yielding

$$\eta_1 = \frac{-1}{g}\tilde{\phi}_{1_t} \quad , \tag{2.9}$$

he free surface boundary condition. Varying L_2 with respect to $\tilde{\phi}_1$ and erforming a partial integration over the propagation space yields

$$-\eta_{1_t} - \nabla_h \cdot (I^{'}_{1,1}\nabla_h\tilde{\phi}_1) + I^{z}_{1,1}\tilde{\phi}_1 = 0 \tag{2.10}$$

Eliminating η_1 between (2.9) and (2.10) and inserting the values of the integrals yields

$$\tilde{\phi}_{1_{tt}} - \nabla_h \cdot (CC_g\nabla_h\tilde{\phi}_1) + (\omega^2 - k^2CC_g)\tilde{\phi}_1 = 0 \tag{2.11}$$

which is the time dependent form of the mild slope equation of Berkhoff (1972). Here,

$$C = \omega/k \quad ; \quad C_g = \partial\omega/\partial k \quad ; \quad \omega^2 = gk\tanh kh. \tag{2.12}$$

Varying L_4 with respect to $(\eta_2 + b_2)$ yields a free surface boundary condition, which may be written as

$$L = \frac{g}{2}(\eta^2 + h^2) + \varepsilon\, I_1 \tilde{\phi}_{1_t} + \varepsilon^2 \{I_2 \tilde{\phi}_{2_t} + (h+\eta)(\phi'_{2_t} - \gamma_2)\}$$

$$+ \varepsilon^2 I_{1,1} \frac{(\nabla_h \tilde{\phi}_1)^2}{2} + \varepsilon^3 \{I_{1,2} \nabla_h \tilde{\phi}_1 \cdot \nabla_h \tilde{\phi}_2 + I_1 \nabla_h \tilde{\phi}_1 \cdot \nabla_\eta \phi'_2\}$$

$$+ \varepsilon^4 \{I_{2,2} \frac{(\nabla_h \tilde{\phi}_2)^2}{2} + I_2 \nabla_h \tilde{\phi}_2 \cdot \nabla_h \phi'_2 + \frac{(\nabla_h \phi'_2)^2}{2} (h-\eta)\}$$

$$+ \varepsilon^2 I^z_{1,1} \frac{(\tilde{\phi}_1)^2}{2} + \varepsilon^3 I^z_{1,2} \tilde{\phi}_1 \tilde{\phi}_2 + \varepsilon^4 I^z_{2,2} \frac{(\tilde{\phi}_2)^2}{2} \qquad (2.6)$$

The integrals I are over the total depth and are defined in Appendix III.A. The I's may be expanded about z=0 in Taylor series according to

$$I = I' + \varepsilon \eta_1 I'' + \varepsilon^2 \{(\eta_2 + b_2) I'' + \eta_1^2 I'''\} + \varepsilon^3 \{2\eta_1 (\eta_2 + b_2) I''' + \eta_1^3 I^{IV}\} + O(\varepsilon^4) \qquad (2.7)$$

as shown in Appendix III.A. Substituting the expansions in (2.6), expanding the remaining appearances of η, and retaining terms to $O(\varepsilon^4)$ leads to the expression

$$L = L_0 + \varepsilon L_1 + \varepsilon^2 L_2 + \varepsilon^3 L_3 + \varepsilon^4 L_4 \,. \qquad (2.8)$$

The individual coefficients L_i are given in Appendix III.B. This ordering has also been utilized by Dysthe (1974) after averaging L over the phase function according to Whitham's method. Serveral properties of (2.8) with respect to the desired governing equations can be mentioned. Since variation with respect to a dependent parameter will reduce the order of L by the order of

$$\delta \int_t \int_{\underline{x}} L \, d\underline{x} \, dt = 0 \tag{2.3}$$

where the integration is over the propagation space $\{x,y,t\}$.

Since we wish to study the spatial evolution of a time-independent wave field, it is sufficient to choose forms for ϕ and η based on a slow-modulation solution of the governing equations, as in Whitham (1967). Consequently, we choose a wave steepness scale ε and modulation scale μ and propose a priori that $\mu \sim \varepsilon^2$. This assumption produces a mild slope approximation in which bottom slope terms and nonlinear terms are isolated from each other, as in Kirby and Dalrymple (1983). We choose ϕ and η according to

$$\phi = \varepsilon f_1(\mu\underline{x},z)\tilde{\phi}_1(\underline{x},t) + \varepsilon^2\{f_2(\mu x,z)\tilde{\phi}_2(\underline{x},t) + \phi_2'(\underline{x},\mu t) - \int \gamma_2(\mu\underline{x},t)dt\} \tag{2.4a}$$

$$\eta = \varepsilon\eta_1(\underline{x},t) + \varepsilon^2\{\eta_2(\underline{x},t) + b_2(\underline{x},\mu t)\} \tag{2.4b}$$

Here, $\tilde{\phi}_1,\eta_1,\tilde{\phi}_2,\eta_2$ correspond to first and second order wavelike components, ϕ_2' is the potential for wave-induced mean flow, b_2 represents the wave-induced set-down, and γ_2 is related to the Bernoulli constant. We remark that in a partial standing wave γ_2 cannot be trivially eliminated by choice of b_2, and that γ_2, b_2 and ϕ_2' may have fast variations as indicated. The quantities f_1 and f_2 are given by

$$f_1 = \frac{\cosh k(h+z)}{\cosh kh} \quad ; \quad f_2 = \frac{\cosh 2k(h+z)}{\sinh^4 kh} \quad ; \quad h = h(\mu\underline{x}) \tag{2.5}$$

Substituting (2.4) in (2.1) and performing the integration results in the expression

III.2 Derivation of the Equations Governing Wave Propagation

We wish to derive the equations governing the forward and backward moving wave components in a partial standing wave, where x is taken as the (positive) direction of travel. Previous derivations of the nonlinear Schrödinger equation for forward scattered waves alone have relied on the WKB formulation and a multiple scale expansion of the governing equations. However, a scheme for providing coupled equations has not been devised using that approach. Here, we will rely instead on a variational formulation using the Lagrangian for irrotational motion of an inviscid fluid, given by Luke (1967). After deriving equations for a general wave motion in two horizontal dimensions (x,y) and time, the results will be specialized to the case of two waves propagating in an anti-parallel direction. The method used here is further discussed in Kirby (1983) and Kirby and Dalrymple (1984) in connection with the problem of wave-current interaction.

III.2.1 The Lagrangian Formulation and Governing Equations

The Lagrangian for irrotational motion is given by (Luke, 1967)

$$L = \int_{-h}^{\eta} \rho\{\phi_t + \frac{1}{2}(\nabla_h\phi)^2 + \frac{1}{2}(\phi_z)^2 + gz\}\, dz \qquad (2.1)$$

Here, $\eta(x,y,t)$ is the instantaneous position of the water surface with respect to still water level $z=0$, and $h(x,y)$ is the local water depth. The potential $\phi(x,y,z,t)$ is related to the fluid velocity according to

$$\underline{u} = \nabla\phi \quad , \qquad (2.2)$$

Further, ∇_h denotes a horizontal gradient vector $\{ \frac{\partial}{\partial x} , \frac{\partial}{\partial y} \}$ and subscripts denote differentiation. The corresponding variational principle is given by

The results mentioned above are based on the assumption that the reflected wave is absent or negligible. This assumption is certainly valid locally in a slowly varying domain; however, a sizeable reflected component may accumulate for waves propagating over long distances or over fairly abrupt obstacles, such as those studied in Chapter II. Liu and Tsay (1983) have developed an iterative scheme based on coupled equations similar to those of Radder (1979), and have shown that the coupled method for forward- and back-scattered waves is capable of producing results in agreement with a finite element solution of Berkhoff's equation, where the entire wavefield is calculated simultaneously (Tsay and Liu (1982)).

In this study, we extend the results of Kirby and Dalrymple (1983) and Liu and Tsay (1983) to study the gradual reflection of Stokes waves by slow depth variations. In addition, the results of Chapter II are incorporated in order to allow for the application of the model to reflection from sand bars and related features. In Section 2, a derivation of the equations governing the evolution of a slowly varying partial standing wave train are derived in order to obtain the nonlinear coupling coefficients between incident and reflected waves. Section 3 then presents a modification of the splitting approach used in Chapter II, which produces the needed set of coupled parabolic equations. In Section 4, we study a special case of waves normally incident on topography varying in one direction, in order to evaluate the effect of neglecting interaction with wave-induced currents which enter the equations at third order. The parabolic approximation is then applied to the study of a two-dimensional problem in Section 5.

Chapter III

On the Gradual Reflection of Weakly-Nonlinear Stokes Waves in Regions with Varying Topography

III.1 Introduction

Various recent studies have explored the application of the parabolic equation method to the problems of wave propagation in a slowly varying domain. In the linear wave approximation, Berkhoff (1972) has provided a second order wave equation governing the surface potential $\hat{\phi}(x,y)$ of a harmonic wave, based on the assumption of modulation length scales smaller than the wave steepness scale. Radder (1979) obtained coupled parabolic equations for forward- and back-scattered waves, where it is assumed that both waves travel at a small angle to a prespecified direction. A model for the forward-scattered wave field alone is then obtained by neglecting the coupling terms. Berkhoff, Booij and Radder (1982) have provided a data set for wave amplitude in an area of waves focussed by a submerged shoal, and have used the data to test Radder's model. Additional results for forward-scattering alone in a linear approximation have been provided by Liu and Mei (1976) and Tsay and Liu (1982). Kirby and Dalrymple (1983) have extended the linear wave approximation to include the effect of cubic nonlinearity for Stokes waves, which leads to a nonlinear Schrödinger equation for the wave amplitude. Kirby and Dalrymple (1984) have tested the nonlinear model in comparison to the data set of Berkhoff, Booij and Radder and have shown a distinct improvement in agreement between model and data in comparison to the results of Radder's model. The nonlinear model has thus been shown to be a relevant addition to the study of combined refraction-diffraction.

marked contrast to the case of edge waves on a plane beach, where the shoreline singularity dominates wave amplification.

II.6. Conclusions

This chapter has provided a general wave equation for linear surface waves in intermediate depth, which extends the range of applicability of the mild-slope approximation by providing for relatively rapid undulations in depth. Deviations from the mean, slowly varying depth must be small in relative amplitude but may be of any arbitrary form. The present results thus extend the previous analytic results for sinusoidal topography, and make it possible to directly handle physically realistic, one- or two dimensional bed-forms.

Although the results of Section 3 show that the small-amplitude theory is able to predict physically realistic results for wave reflection over bed undulations with amplitudes as large as 32 percent of the mean depth, it is expected that some limitation to the present theory would occur with increasingly higher bed forms. The limitations of the small amplitude theory have been investigated by Dalrymple and Kirby (1984), using a boundary integral approach for bottom undulations of arbitrary height. However, the results of Section 5 indicate that fairly large bottom variations may be treated with a reasonable degree of accuracy.

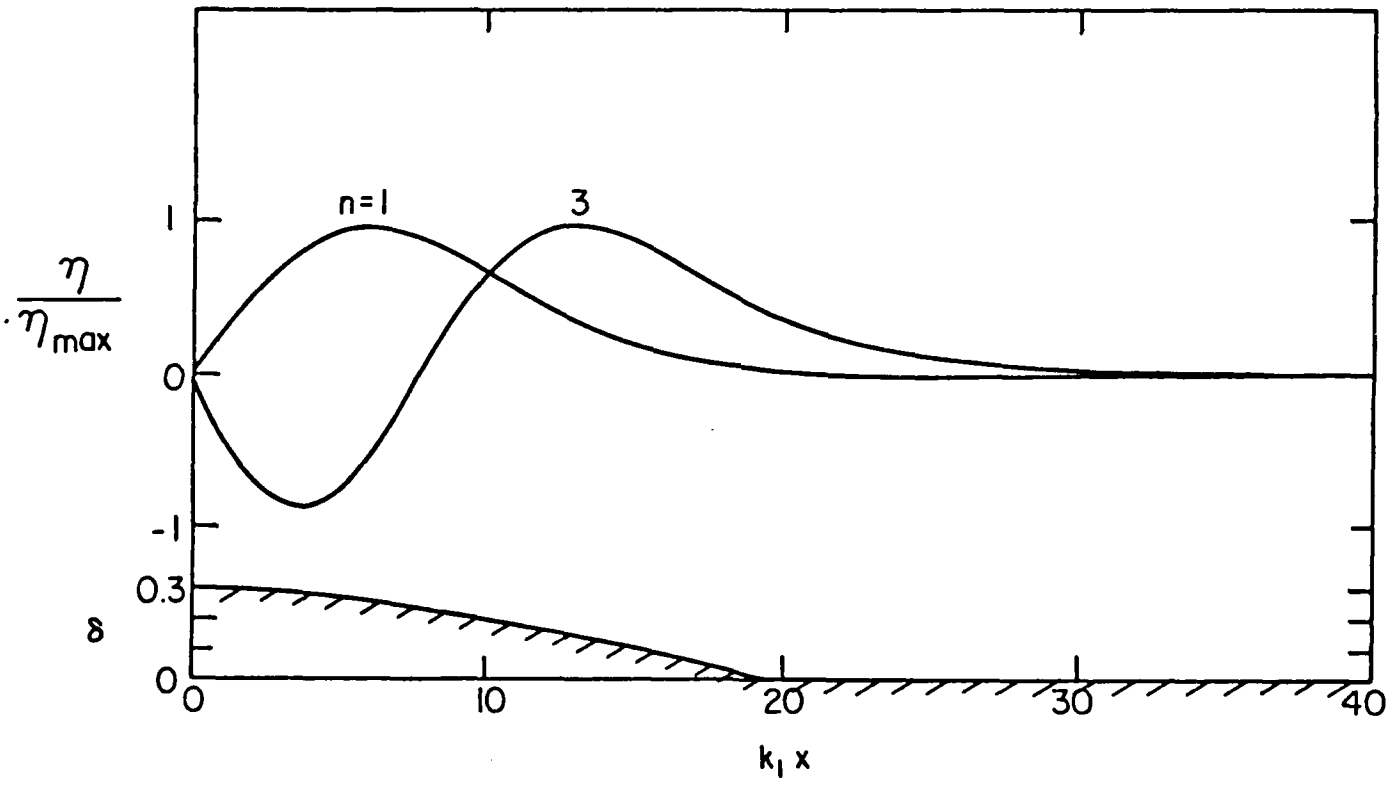

b) anti-symmetric modes n = 1, 3

Figure II.10. Continued

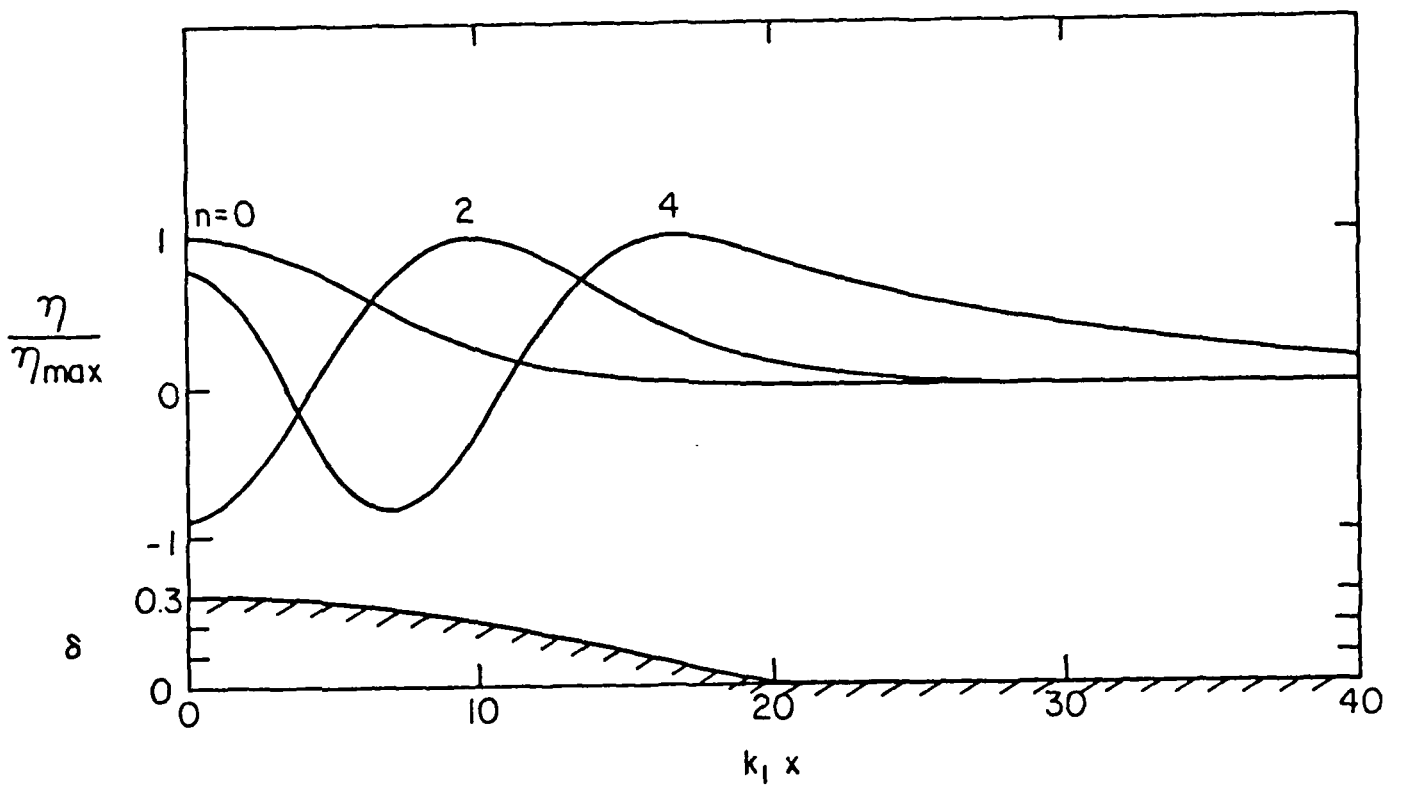

a) symmetric modes n = 0, 2, 4

Figure II.10. Surface profiles of trapped waves for cosine topography, $k_1L = 20$, $D/h_1 = 0.3$.

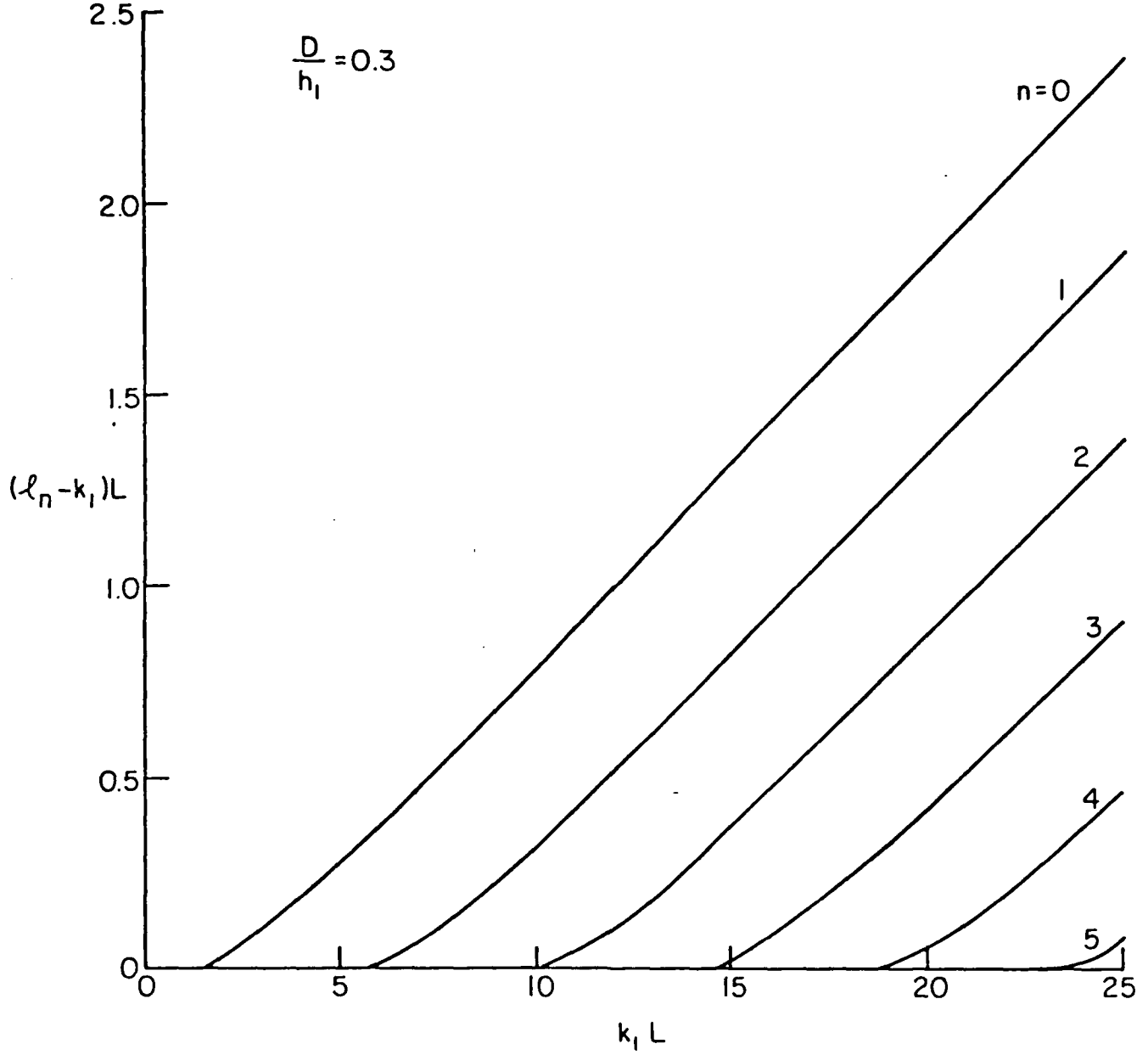

Figure II.9. Dispersion relation for $\delta = D\cos(\pi x/2L)$ topography. $D/h_1 = 0.3$, $h_1 = 1$ m

The symmetric and anti-symmetric cases correspond to even and odd mode numbers n, respectively. As in the previous example, the wavenumber ℓ along the ridge must be $> k_1$ away from the ridge, while the presence of regions of constant depth to either side of the ridge implies the existence of cutoff conditions for the highest mode number.

Numerical results were obtained for the particular case of $D/h_1 = 0.3$. The curves representing the dispersion relation are given in Figure II.9. These results were obtained by varying L and using a fixed depth $h_1 = 1$, for which $k_1 = 1.2051$. As expected, the number of trapped modes increases with increasing L (increasing ξ^*, above). The present computations are for a fairly large amplitude bottom deviation; decreasing the amplitude D would have the effect of decreasing the possible number of trapped modes at a fixed value of L, due to the concurrent reduction in the ξ^* parameter.

Plots of the surface profiles for symmetric modes and anti-symmetric modes are given in Figures II.10a and II.10b, respectively, for the case of $k_1 L = 20$. In contrast to the results of McIver and Evans (1984), where the depth at large x goes to infinity, it is seen that the maximum amplitude along a given mode profile does not necessarily occur at the antinode in shallowest water, but instead typically occurs at an antinode nearer to the location of the turning point for the profile in question. This effect was also noted by Dolan (1983), who calculated edge wave modes over real profiles taken from the Chesapeake Bay. The profiles studied by Dolan typically had fairly steep foreshores and then were extremely flat out to the region of the caustic (turning point) for the edge wave mode. In both that case and the present case, the effect of shoaling between the line of symmetry (or shoreline) and the region of the caustic is fairly mild, and the maximum amplification occurs near the caustic due to the refractive singularity. These effects are in

equivalently, $0 < D/h_1 < 0.4$. This result indicates that the present small-amplitude bottom variation theory is reasonably accurate in comparison to the mild-slope theory for bottom variations on the order of 0-40% of the mean depth, even when the deviation δ is nearly constant and extends over a large physical distance. It is therefore understandable that agreement between data and theory was good for the $D/h = 0.32$ case in Section 3.

As a final example, we consider the waves trapped over a ridge with continuous profile

$$\delta(x) = \begin{cases} D\cos(\pi x/2L) & |x| \leq L \\ 0 & |x| > L \end{cases} \tag{5.15}$$

and with h = constant. The dispersion relation and surface profiles are obtained numerically using (5.2) and the formulation of Kirby et al, without any coordinate stretching. Due to symmetry, the solution is obtained only over the region $0 \leq x \leq x_M$, with the boundary condition

$$\psi(x_M) = 0 \tag{5.16}$$

imposed as an approximation of the requirement that $\psi \to 0$ as $x \to \infty$. The resulting trapped waves may be symmetric or antisymmetric about $x = 0$; the approximate boundary conditions are:

$$\begin{aligned} &\psi(0) = 0 \quad ; \text{ anti-symmetric case} \\ &\psi_x(0) = 0 \quad ; \text{ symmetric case} \end{aligned} \tag{5.17}$$

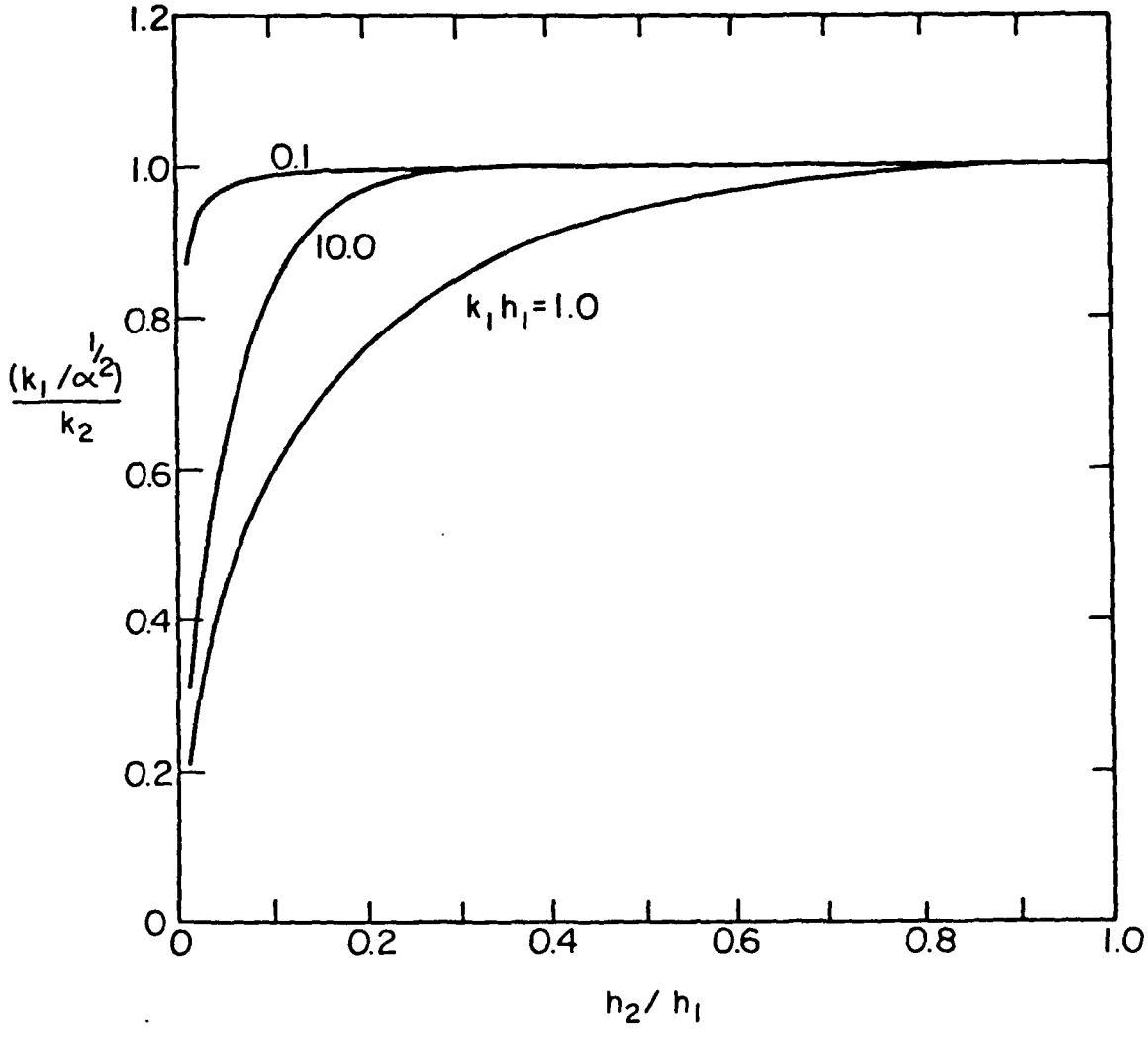

b) Ratio of $k_1/(\alpha)^{1/2}$ to k_2; α from present theory

Figure II.8. Continued

III.2.2 Explicit Results for Partial Standing Waves

We now wish to construct parabolic approximations for the amplitude of two wave components of the same frequency ω and with an angle of 180° between the assumed direction of the wavenumber vectors. We choose

$$\tilde{\phi}_1 = \phi_1^+ + \phi_1^-$$

$$= \frac{-ig}{2\omega} A(\mu x,\mu y,\mu t)\, E_+ + * \frac{-ig}{2\omega} B(\mu x,\mu y,\mu t)\, E_- + * \tag{2.16}$$

where

$$E_+ = e^{i(kx-\omega t)} \quad ; \quad E_- = e^{i(-kx-\omega t)} \tag{2.17}$$

and where * denotes the complex conjugate of the preceeding term. The propagation direction of ϕ^+ is oriented with the +x direction. Using this splitting and the equations of the preceeding subsection, we obtain

$$\eta_1 = \frac{A}{2} E_+ + * + \frac{B}{2} E_- + * + O(\mu) \tag{2.18}$$

$$\tilde{\phi}_2 = \frac{-3i\omega}{16} A^2 E_+^2 + * \frac{-3i\omega}{16} B^2 E_-^2 + * + O(\mu) \tag{2.19}$$

$$\eta_2 = \frac{k}{4} \frac{(\cosh 2kh - 2)}{\sinh 2kh} \cdot \{A^2 E_+^2 + B^2 E_-^2 + *\} - \frac{I_2''}{g} \tilde{\phi}_{2_t}$$

$$= \frac{k}{8} \frac{\cosh kh(\cosh 2kh+2)}{\sinh^3 kh} \{A^2 E_+^2 + * B^2 E_-^2 + *\} + O(\mu) \tag{2.20}$$

$$b_2 = \frac{-1}{g} \phi'_{2_t} - \frac{k(|A|^2+|B|^2)}{2\sinh 2kh} + \frac{k\cosh 2kh}{2\sinh 2kh} (AB^* E_+ E_-^* + *) \tag{2.21}$$

The third term in (2.21) corresponds to a rapid standing variation at cos(2kx) corresponding to the envelope of the partial standing wave. Further,

$$\gamma_2 = \frac{-gh(2\cosh 2kh-1)}{2\sinh 2kh}\{ABE_+E_- + *\} \tag{2.22}$$

which represents a spatially slowly varying oscillation at cos(2ωt). We remark that γ_2 may not be eliminated by choice of b_2, in contrast to the progressive wave problem. Elimination of $(\eta_2 + b_2)$ between (2.13) and (2.14) yields the forced wave equation for the $O(\varepsilon^2)$ mean motion:

$$\phi_{2_{tt}}' - \nabla_h\cdot(gh\nabla_h\phi_2') = \frac{g^2}{2\omega}(k|A|^2 - k|B|^2)_x - \frac{gk}{2\sinh 2kh}(|A|^2 + |B|^2)_t$$

$$= \frac{gk\cosh 2kh}{2\sinh 2kh}(AB^*E_+E_- + *)_t \tag{2.23}$$

The third term in the r.h.s. of (2.23) indicates that spatially fast (~2kx) adjustments in b_2 and ϕ_2' will occur in response to slow temporal changes in the amplitude of ϕ_1^+ or ϕ_1^-.

Substitution of (2.16) - (2.21) in the expression for N.L.T. yields the result

$$\begin{aligned}
\text{N.L.T.} = &-2\omega\left\{k\phi_{2_x}' - \frac{k^2}{2\omega\cosh^2 kh}\phi_{2_t}'\right\}\phi_1^+ \\
&+ 2\omega\left\{k\phi_{2_x}' + \frac{k^2}{2\omega\cosh^2 kh}\phi'_{2_t}\right\}\phi_1^- \\
&- \omega^2k^2D_1(|A|^2\phi_1^+ + |B|^2\phi_1^-) \\
&- \omega^2k^2D_2(|B|^2\phi_1^+ + |A|^2\phi_1^-) \\
&+ \text{terms proportional to } E^3
\end{aligned} \tag{2.24}$$

In the following, a Fourier decomposition will eliminate terms αE^3, which would have been taken care of by inclusion of $\tilde{\phi}_3$. The coefficients D_1 and D_2 are given by

$$D_1 = \frac{\cosh 4kh + 8 - 2\tanh^2 kh}{8\sinh^4 kh} \tag{2.25}$$

$$D_2 = \frac{-(16 \sinh^4 kh + 4 \tanh^2 kh)}{8\sinh^4 kh} \tag{2.26}$$

and have the deepwater asymptotes ($kh \to \infty$) of 1 and -2, respectively, in agreement with the results of Benney (1962) and Roskes (1976). Noting that the l.h.s. of (2.15) is a linear operator on $\tilde{\phi}_1$, we then arrive at decoupled equations for ϕ_1^+ and ϕ_1^- given by

$$\phi_{1_{tt}}^+ - \nabla\cdot(CC_g\nabla\phi_1^+) + (\omega^2 - k^2CC_g)\,\phi_1^+ + 2\omega\left\{k\phi_{2_x}' - \frac{k^2}{2\omega\cosh 2kh}\phi_{2_t}'\right\}\phi_1^+$$

$$+ \omega^2k^2(D_1|A|^2 + D_2|B|^2)\,\phi_1^+ = 0 \tag{2.27a}$$

$$\phi_{1_{tt}}^- - \nabla\cdot(CC_g\nabla\phi_1^-) + (\omega^2 - k^2CC_g)\,\phi_1^- - 2\omega\left\{k\phi_{2_x}' + \frac{k^2}{2\omega\cosh^2 kh}\phi_{2_t}'\right\}\phi_1^-$$

$$+ \omega^2k^2(D_1|B|^2 + D_2|A|^2)\,\phi_1^- = 0 \tag{2.27b}$$

The change in sign of the terms $k\phi_{2_x}'$ is related to the different directions of propagation of ϕ_1^+ and ϕ_1^-. Since D_2 is always <0, while D_1 is >0, it is apparent that the presence of a reflected wave component ϕ_1^- weakens the effect of nonlinear self-interaction in the incident wave component. Parabolic approximations governing A and B follow by neglecting time dependence for

purely harmonic motion, and further by assuming that $O(|A_{xx}|)<<O(k|A_x|)$ as in Kirby and Dalrymple (1983). The decoupled parabolic equations are then given by (following the method of Kirby and Dalrymple (1983))

$$2ikCC_gA_x + 2k(k-k_0)CC_gA + i(kCC_g)_xA +$$

$$+(CC_gA_y)_y - \omega^2k^2\left(D_1|A|^2 + D^2|B|^2 + \frac{2}{\omega k}(\phi_2')_x\right) A=0 \qquad (2.28)$$

and

$$2ikCC_gB_x - 2k(k-k_0)CC_gB + i(kCC_g)_xB -$$

$$-(CC_gB_y)_y + \omega^2k^2\left(D_1|B|^2 + D^2|A|^2 - \frac{2}{\omega k}(\phi_2')_x\right) B=0 \qquad (2.29)$$

where k_0 is a constant wavenumber defining the reference phase function $k_0x - \omega t$. These equations are sufficient for modelling the propagation of the individual components ϕ_1^+ and ϕ_1^- including their nonlinear interaction; however, we have not yet achieved a coupling capable of predicting the appearance of a gradually reflected component ϕ_1^-. This coupling is achieved in the following section.

III.2.3 Effect of Reflected Wave and Mass Transport on the Nonlinear Dispersion of the Incident Wave

The effect of reflected wave components and induced flow on the third order dispersion of the incident wave may be examined explicitly in the case of one directional propagation over topography varying only in the direction of propagation. In this case, we may integrate (2.23) after neglecting time dependence to obtain

$$\phi'_{2_x} = -\frac{gk}{2\omega h}\left(|A|^2 - |B|^2\right) + \text{Constant} \tag{2.30}$$

where the integration constant represents an externally imposed flow which is set to zero. Assuming that $|B| < |A|$; i.e., that $\tilde{\phi}_1^-$ represents a small wave arising due to reflection, and taking $R = |B|/|A|$ to represent a reflection coefficient, the governing equation for the incident wave may be written as

$$2ikCC_gA_x + i(kCC_g)_xA - \omega^2k^2D^*|A|^2A = 0 \tag{2.31}$$

where

$$D_* = D_1 + D_2R^2 - \frac{g}{\omega^2 h}(1 - R^2) \tag{2.32}$$

The last term in D_* represents the effect of wave-induced return flow balancing the shoreward mass flux of the waves. Since $D_2 < 0$ for all kh, the generation of a reflected component reduces the dispersive effect of nonlinearity. Conversely, incrasing reflection tends to reduce the effect of the wave-induced return current, as the mass flux of the reflected wave tends to balance out the flux of the incident wave.

Figure III.1 gives plots of $D^*(kh, R)$ for a range $0 \leq R \leq 1$, with and without current effects included. It is noted that, for all reasonably small values of kh, the mean current has a noticable effect on D^*, with the effect becoming pronounced for $kh < \sim 4$. It is also apparent that the reflected wave can act to entire cancel the amplitude dispersion of the incident wave, with the critical value being given by

$$R_c = \left\{\frac{\left(\frac{g}{\omega^2 h} - D_1\right)}{\left(\frac{g}{\omega^2 h} + D_2\right)}\right\}^{1/2} \tag{2.33}$$

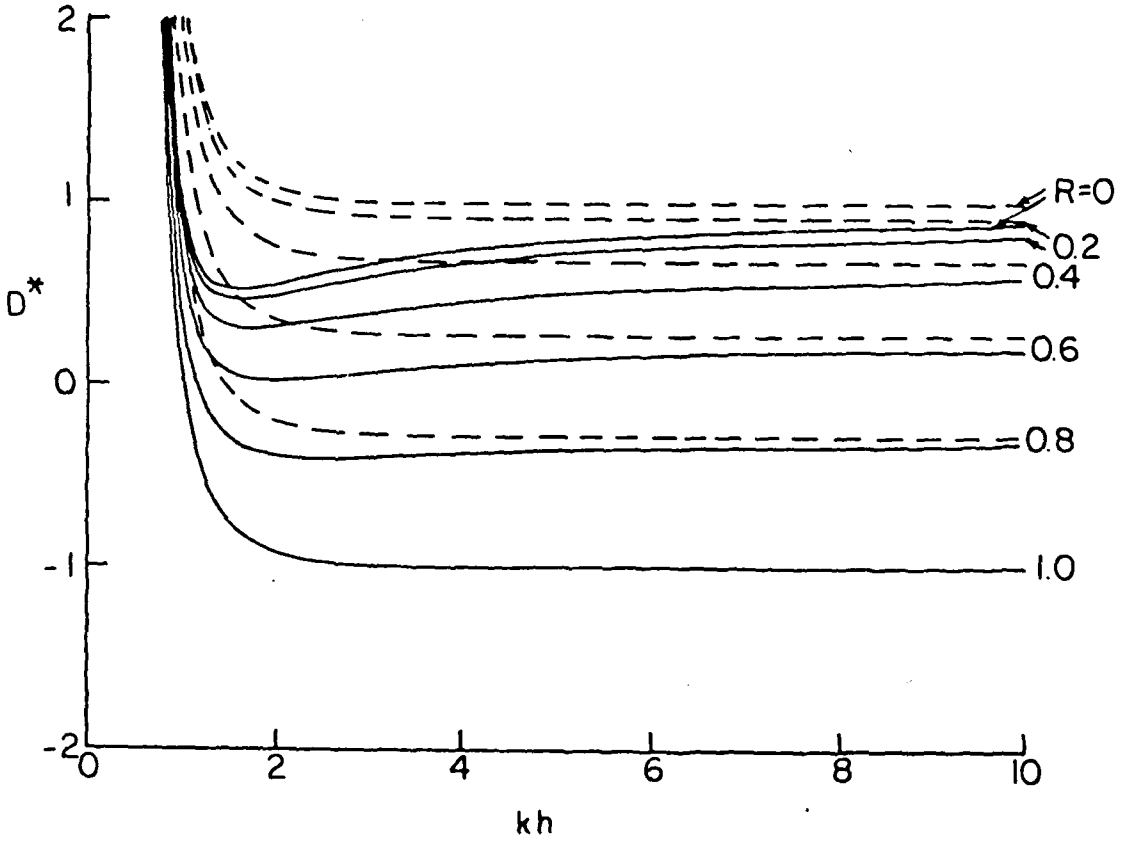

Figure III.1 Variation of D* with kh and reflection coefficient R.———, including wave-induced return flow; ---, neglecting wave-induced return flow

Neglecting current effects, this becomes

$$R_c = \left\{ - \frac{D_1}{D_2} \right\}^{1/2} \tag{2.34}$$

which is defined for all kh and $\to 2^{-1/2}$ as $kh \to \infty$. When current is included, R_c is undefined for $kh \leq 0.649$; the deepwater asymptotic value is unaffected. A plot of R_c with and without currents is given in Figure III.2. Since it is apparent that the effect of the wave induced flow can significantly alter the coefficient of the nonlinear term for values of kh small enough to give significant depth change effects over a short spatial scale, we investigate the effect of retaining or dropping the current in a one-dimensional example in Section 4, eliminating ϕ'_{2_x} as was done here. The general problem of coupling between A, B and ϕ'_{2_x} in two dimensions is left to a subsequent study.

III.2.4 Extension to the Case of Rapid Bed Undulations

The theory derived to this point is limited in application to waves propagating over mild bed slopes, with slope parameter μ presumed to be of $O(\varepsilon^2)$ in order to separate nonlinear and bottom slope effects. Reflections from such mild slopes are likely to be extremely weak in intermediate water depth. Therefore, it is desirable to incorporate the rapid undulation, small amplitude bed features in the manner of Chapter II. We thus add a bed amplitude parameter $k\delta$ to the list of $O(\mu)$ parameters. If we retain the scaling assumptions used to this point in Chapter III terms like

$$\delta A, \ \delta_x A, \text{ etc.}$$

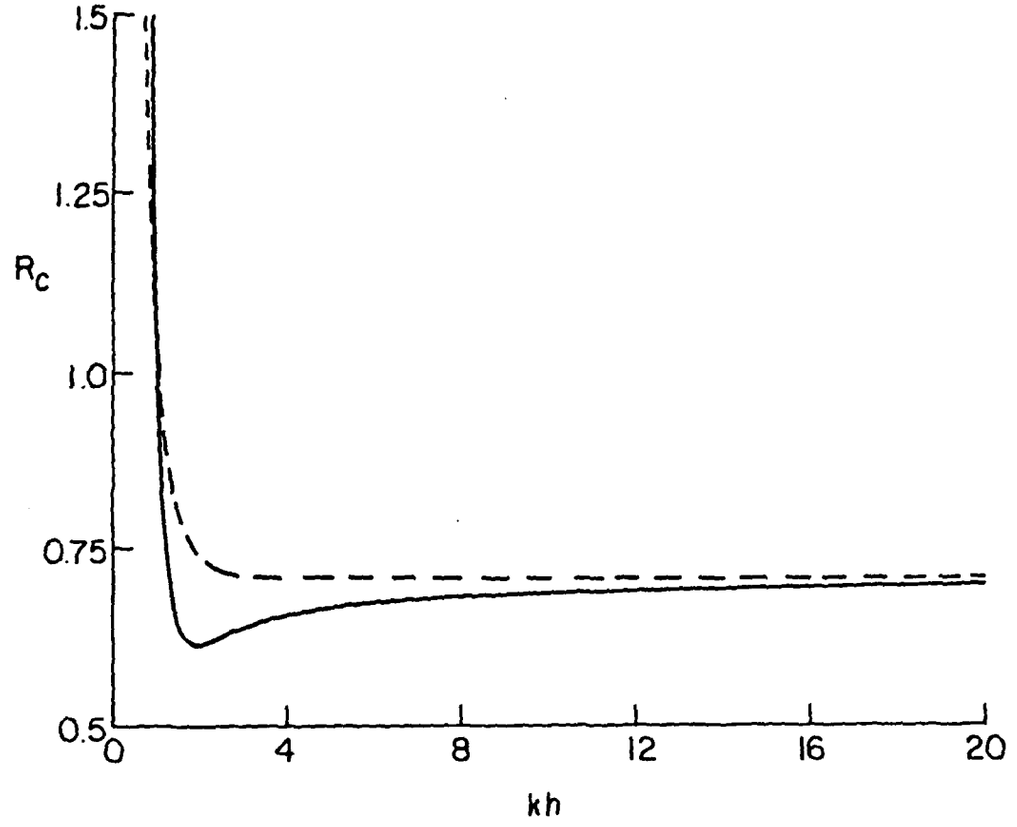

Figure III.2 Critical reflection coefficient R_c for D*=0. ——,--- as in Figure III.1

will still be of $O(\varepsilon^3)$; the addition of this feature will not affect the amplitude dispersion and interaction with the wave-induced mean flow at the highest order of magnitude (ε^3) retained here. We therefore consider the extension of the linear wave Lagrangian formulation to incorporate the features of Chapter II. The nonlinear terms are unaffected and may be retained intact from Section III.2.2.

Defining the total water depth as in Chapter II, we have

$$h' = h - \delta \tag{2.35}$$

where h varies slowly with length scale μ, and where δ may vary rapidly but has amplitude scale μ. Following (2.1), the Lagrangian for the inviscid motion may be written as

$$L = \int_{-h'}^{\eta} \rho \left\{ \phi_t + \frac{1}{2} (\nabla_h \phi)^2 + \frac{1}{2} (\phi_z)^2 + gz \right\} dz \tag{2.36}$$

We now expand the Lagrangian about $z = -h$ and retain the $O(\varepsilon^2)$ contributing to the linear motion.

$$L = \frac{g\eta^2}{2} + \eta\phi_t \Big|_{z=0} + \int_{-h}^{0} \frac{(\nabla_h \phi)^2}{2} dz - \frac{(\nabla_h \phi)^2}{2} \delta \Big|_{z=-h}$$

$$+ \int_{-h}^{0} \frac{(\phi_z)^2}{2} dz - \frac{(\phi_z)^2}{2} \delta \Big|_{-h} \tag{2.37}$$

We now introduce

$$\phi = f_1(\mu \underline{x}, z)\, \tilde{\phi}_1(\underline{x}, t) \tag{2.38}$$

where f_1 is given in (2.5). Making the substitutions and integrating gives

$$L = \frac{g\eta^2}{2} + \eta\tilde{\phi}_t + \left(\frac{CC_g}{g}\right)\frac{(\nabla_h\tilde{\phi})^2}{2} + \left(\frac{\omega^2 - k^2CC_g}{g}\right)\frac{\tilde{\phi}^2}{2}$$

$$- \frac{\delta}{\cosh^2 kh}\frac{(\nabla_h\tilde{\phi})^2}{2} \qquad (2.39)$$

Taking variations and eliminating η leads to the modified wave equation (II.2.11),

$$\tilde{\phi}_{tt} - \nabla_h\cdot(CC_g\nabla_h\tilde{\phi}) + (\omega^2 - k^2CC_g)\,\tilde{\phi} + \frac{g}{\cosh^2 kh}\nabla_h\cdot(\delta\nabla_h\tilde{\phi}) = O(\mu^2) \qquad (2.40)$$

The nonlinear model follows, to $O(\varepsilon^3)$, by adding the N.L.T. terms (2.24) to the modified equation (2.40).

III.3 The Coupled Parabolic Equations

The desired set of coupled equations is derivable in a large number of ways (see McDaniel (1975), Corones (1975), Radder (1979) and Liu and Tsay (1983) for examples) involving the application of a splitting matrix to the second order wave equation. We retain the added term for bed undulations derived above for generality. Restricting attention to harmonic waves and substituting

$$\tilde{\phi}_1 = \hat{\phi}e^{-i\omega t} \qquad (3.1)$$

into (2.15), we write

$$(\hat{\phi})_{xx} + p^{-1}p_x(\hat{\phi})_x + \gamma^2\hat{\phi} = N_1\hat{\phi} + N_2\hat{\phi} \qquad (3.2)$$

where, to leading order

$$p = CC_g - \frac{4\omega\Omega'\delta}{k} \tag{3.3a}$$

$$p^{-1} = (CC_g)^{-1}\left[1 + 4\left(\frac{\Omega'}{C_g}\right)\delta\right] + O(\mu^2) \quad , \tag{3.3b}$$

$$\Omega' = gk/4\omega\cosh^2 kh \ , \tag{3.3c}$$

$$\gamma^2\hat{\phi} = k^2\left\{\left(1 + 4\left(\frac{\Omega'}{C_g}\right)\delta\right)\hat{\phi} + \frac{1}{k^2 CC_g}\left(CC_g\hat{\phi}_y\right)_y - \frac{4}{k^2}\left(\frac{\Omega'}{C_g}\right)\left(\delta\hat{\phi}_y\right)_y \right. , \tag{3.3d}$$

$$N_1 = \frac{\omega^2 k^2}{CC_g}\left(D_1|A|^2 + D_2|B|^2 + \frac{2}{\omega k}\left(\phi_2'\right)_x\right) \ , \tag{3.4a}$$

and

$$N_2 = \frac{\omega^2 k^2}{CC_g}\left(D_1|B|^2 + D_2|A|^2 - \frac{2}{\omega k}\left(\phi_2'\right)_x\right) \tag{3.4b}$$

We remark that the pseudo-operator γ is constructed without isolating a refraction factor k/k_0, alleviating the need for making the assumption that

$$1 - \left(\frac{k}{k_0}\right)^2 << 1 \tag{3.5}$$

when performing the binomial expansion of the pseudo-operator (Liu and Tsay, 1983). This assumption may be violated drastically for waves propagating through regions with large depth variations.

We follow the heuristic scheme of Chapter II for obtaining the parabolic equations. Let

$$\hat{\phi}_x^- = i\gamma\hat{\phi} + F + \alpha N_1\hat{\phi}^+ \tag{3.6a}$$

$$\hat{\phi}_x^- = -i\gamma\hat{\phi}^- - F + \beta N_2\hat{\phi}^- \tag{3.6b}$$

where F, α, and β are undetermined. α and β are chosen so as to eliminate nonlinear terms from the coupling term F, leading to equations of the form of (2.28-29). Repeated substitution of (3.6) in (3.2) then leads to

$$\alpha = -\beta = -i/2k \tag{3.7a}$$

and

$$F = -\left\{\frac{(kCC_g)_x}{2kCC_g} - \left(\frac{\Omega'}{C_g}\right)\delta_x\right\}(\hat{\phi}^+ - \hat{\phi}^-) \tag{3.7b}$$

where we have retained terms only to $O(\mu,\varepsilon)$ and have used the fact that

$$CC_g\{N_1\hat{\phi}^+ , N_2\hat{\phi}^-\}_x \tilde{=} ikCC_g\{N_1\hat{\phi}^+ , -N_2\hat{\phi}^-\} + O(\varepsilon^3,\mu) \tag{3.8a}$$

and

$$(CC_g)_x\{N_1\hat{\phi}^+ , N_2\hat{\phi}^-\} \tilde{=} O(\varepsilon^3,\mu) \tag{3.8b}$$

The resulting coupled parabolic equations are then given by

$$\hat{\phi}^+_x - ik\hat{\phi}^+ - \frac{i}{2kCC_g}(CC_g\hat{\phi}^+_y)_y + \frac{(kCC_g)_x}{2kCC_g}(\hat{\phi}^+ - \hat{\phi}^-) - 2ik\left(\frac{\Omega'}{C_g}\right)\delta\hat{\phi}^+ + \frac{2i}{k}\left(\frac{\Omega'}{C_g}\right)(\delta\tilde{\phi}^+_y)_y$$

$$- \left(\frac{\Omega'}{C_g}\right)\delta_x(\hat{\phi}^+ - \hat{\phi}^-) + \frac{i}{2k}N_1\hat{\phi}^+ = 0 \tag{3.9}$$

and

$$\hat{\phi}^-_x + ik\hat{\phi}^- + \frac{i}{2kCC_g}(CC_g\hat{\phi}^-_y)_y - \frac{(kCC_g)_x}{2kCC_g}(\hat{\phi}^+ - \hat{\phi}^-) + 2ik\left(\frac{\Omega'}{C_g}\right)\delta\hat{\phi}^- - \frac{2i}{k}\left(\frac{\Omega'}{C_g}\right)(\delta\hat{\phi}^-_y)_y$$

$$+ \left(\frac{\Omega'}{C_g}\right)\delta_x(\hat{\phi}^+ - \hat{\phi}^-) - \frac{i}{2k}N_2\hat{\phi}^- = 0 \tag{3.10}$$

Equations of the form (2.28-29) are recovered by making the substitutions

$$\hat{\phi}^+ = \frac{-ig}{\omega}Ae^{ik_0x} \quad ; \quad \hat{\phi}^- = \frac{-ig}{\omega}Be^{-ik_0x} \tag{3.11}$$

yielding

$$2ikCC_gA_x + 2k(k-k_0)\,CC_gA + (CC_gA_y)_y + 2\omega\Omega'\,[2k\delta - i\delta_x]A - \frac{4\omega\Omega'}{k}(\delta A_y)_y$$

$$+ i(kCC_g)_x\,A - CC_gN_1A = \{i(kCC_g)_x - 2i\omega\Omega'\delta_x\}\,Be^{-2ik_0x} \qquad (3.12)$$

nd

$$2ikCC_gB_x - 2k(k-k_0)\,CC_gB - (CC_gB_y)_y - 2\omega\Omega'\,[2k\delta + i\delta_x]\,B + \frac{4\omega\Omega'}{k}(\delta B_y)_y$$

$$+ i(kCC_g)_x\,B + CC_gN_2B = \{i(kCC_g)_x - 2i\omega\Omega'\delta_x\}\,Ae^{2ik_0x} \qquad (3.13)$$

Equations (3.12-13) may be used in an iterative fashion to calculate the evolution of the amplitude envelopes A and B. The numerical scheme used in subsequent sections is based on the Crank-Nicolson method, with each equation being solved for the entire domain using the scheme of Yue and Mei (1980), after which iteration between the equations is performed according to the method provided by Liu and Tsay (1983). Details are thus omitted.

III.4 Effect of Mass Transport Terms on Nonlinear Reflection: Normal Incidence on 1-D Topography

As a test of the effect of nonlinearity on the partial reflection process, we first study the reflection of normally incident waves propagating over a continuous, one-dimensional region of slowly varying depth. This reduction of the problem allows for the direct integration of the forced wave equation (2.23) as given by (2.30). Neglect of the integration constant forces the wave induced return flow to balance the net mass transport, and is

thus consistent with the situation of wave-tank experiments. Further, we remark that the generation of free-long waves would be absent from the problem due to the lack of wave-like modulations in the amplitude envelopes.

The choice of computational examples which exhibit significant reflection over a short spatial scale is difficult in this problem, since water depth would have to be relatively shallow in order for an isolated topographic variation with an extent of one to two wavelengths to have a significant effect on the incident wave. For example, the numerical example chosen by Liu and Tsay (1983) was run for a water depth at infinity corresponding to $kh=0.42$. The range of admissible waveheights yielding an Ursell parameter of a permissible size for the Stokes theory to be valid is thus severely constrained. Likewise, the linear transition studies by Booij (1983) covered a range of depths corresponding to $0.2 \leq kh \leq 0.6$, again too small to be of particular use.

For the purposes of this study we have chosen to consider the case of reflection from an isolated patch of sinusoidally undulating topography as studied recently by Davies and Heathershaw (1984) and Mei (1985) as well as in Chapter II.

The topography is given by

$$h'(x) = \begin{cases} h_1 & ; \quad x<0 \\ h_1 - D\sin(2\pi x/\ell) & ; \quad 0 \leq x \leq n\ell \\ h_1 & ; \quad x>n\ell \end{cases} \tag{4.1}$$

where ℓ is the ripple length and n the number of ripples. The topography is illustrated in Figure III.3.

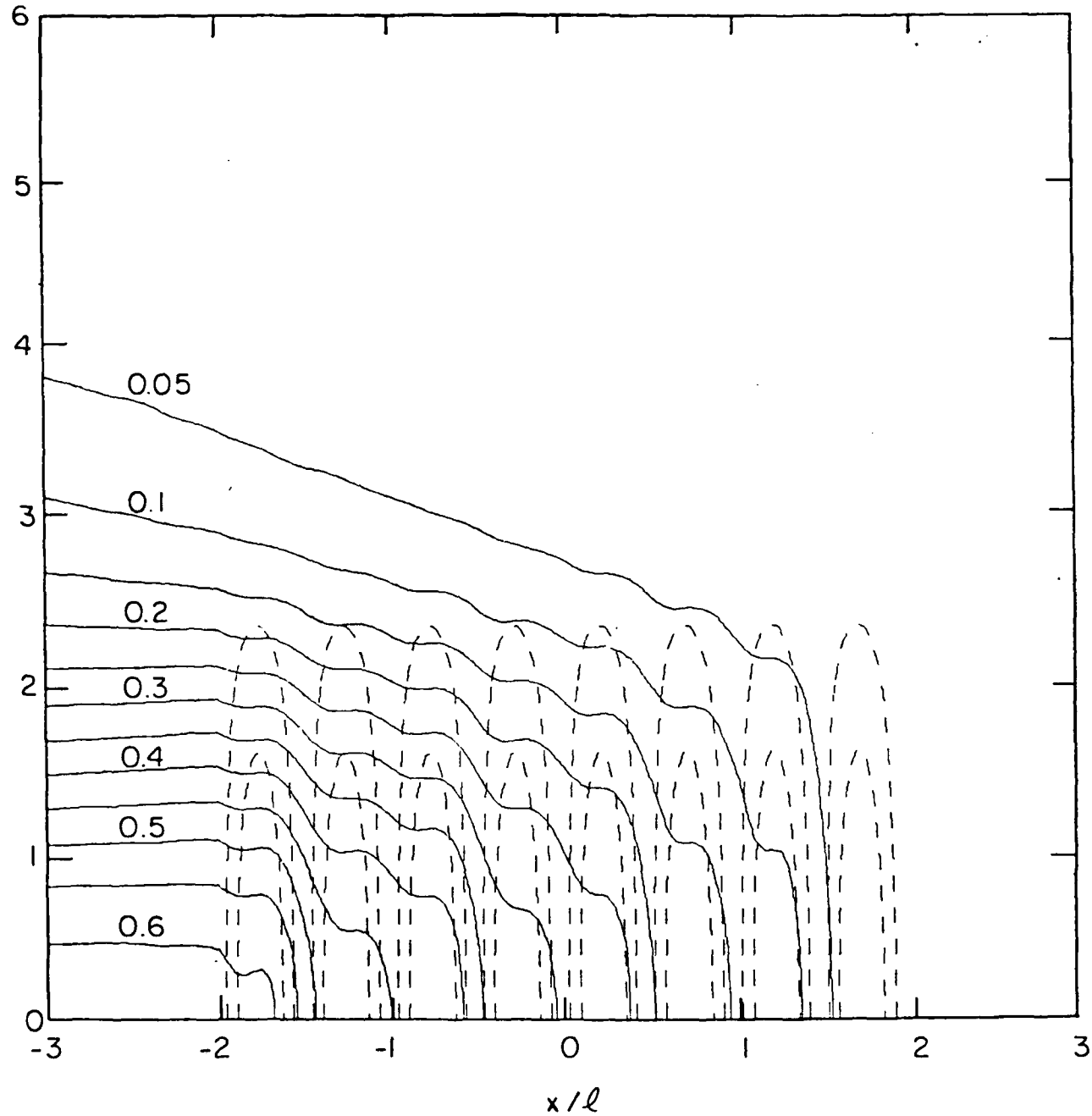

b) $|B|/A_o$

Figure III.8. Continued

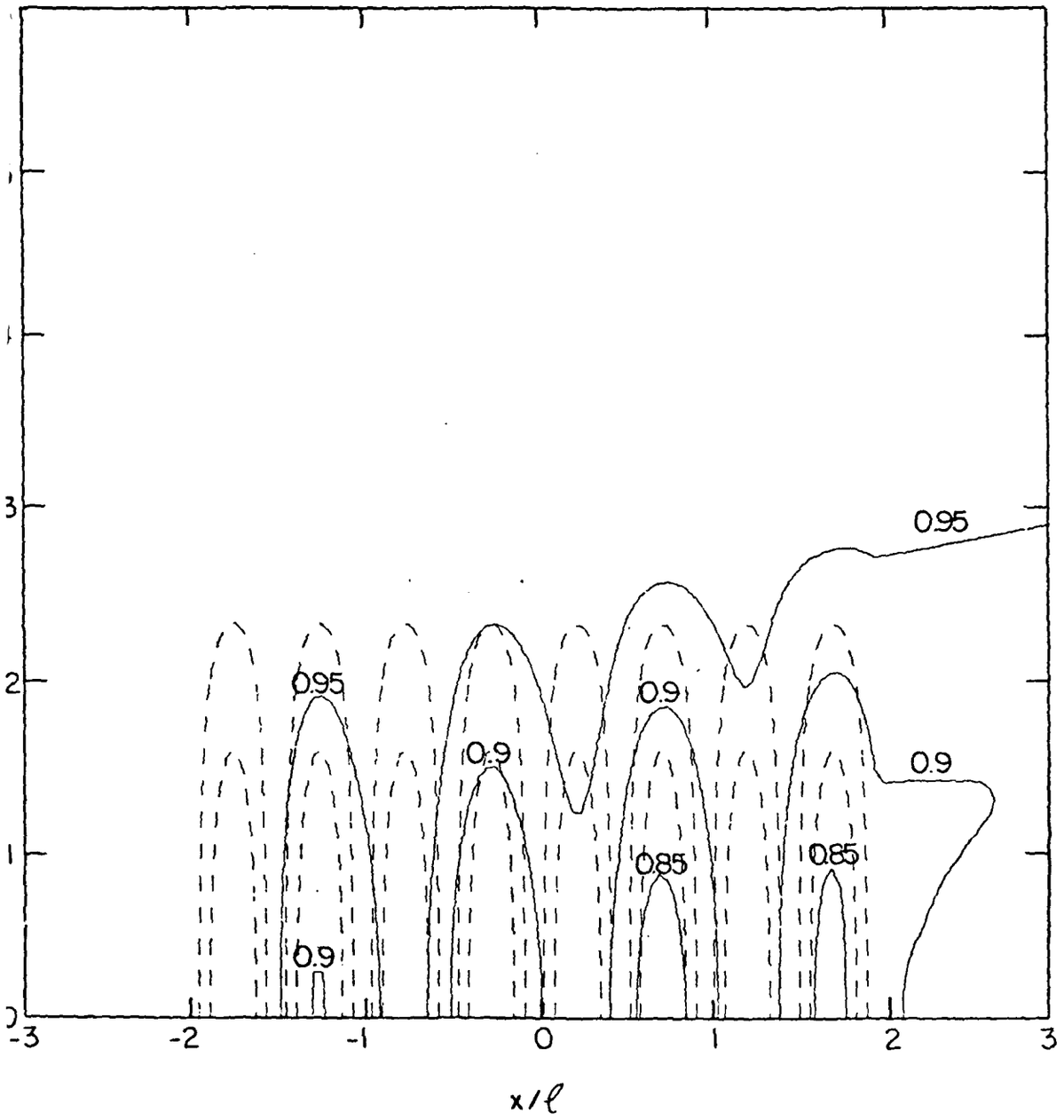

a) $|A|/A_o$

Figure III.8. Normalized amplitude contours: nonlinear wave
—— amplitude contours; --- bottom contours $\delta' = \delta/h_1$

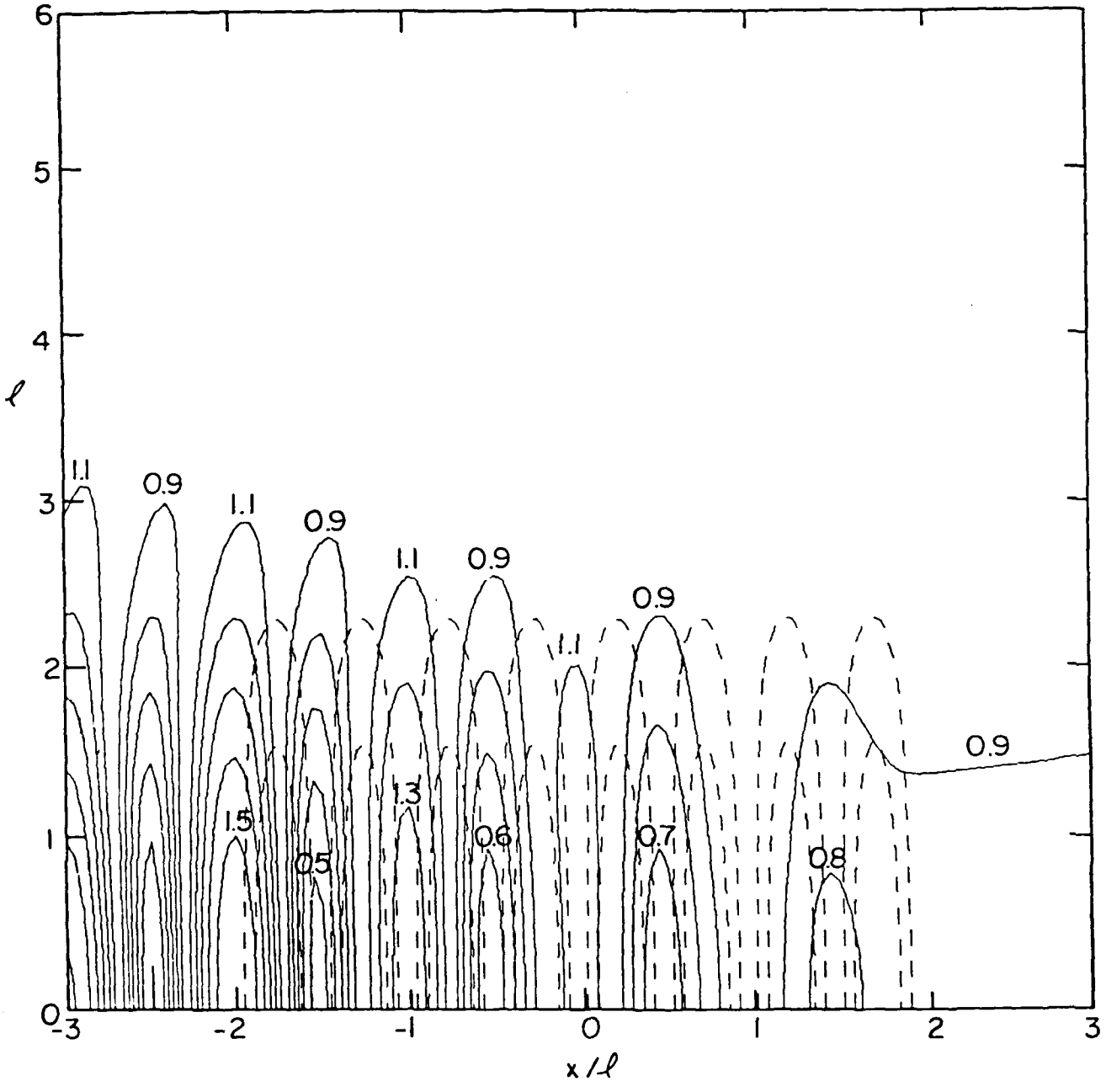

c) $|n|/A_o$

Figure III.7. Continued

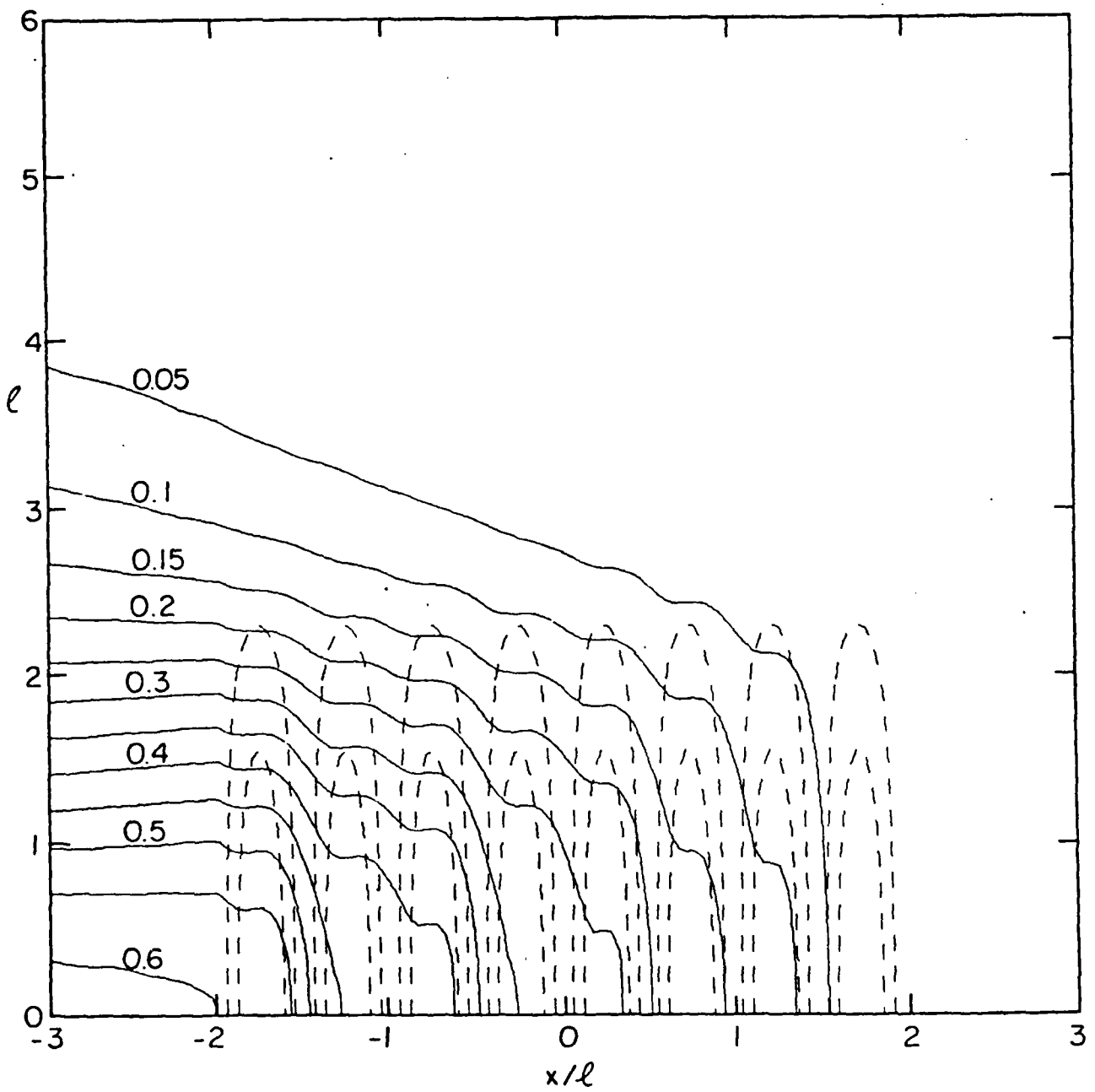

b) $|B|/A_o$

Figure III.7. Continued

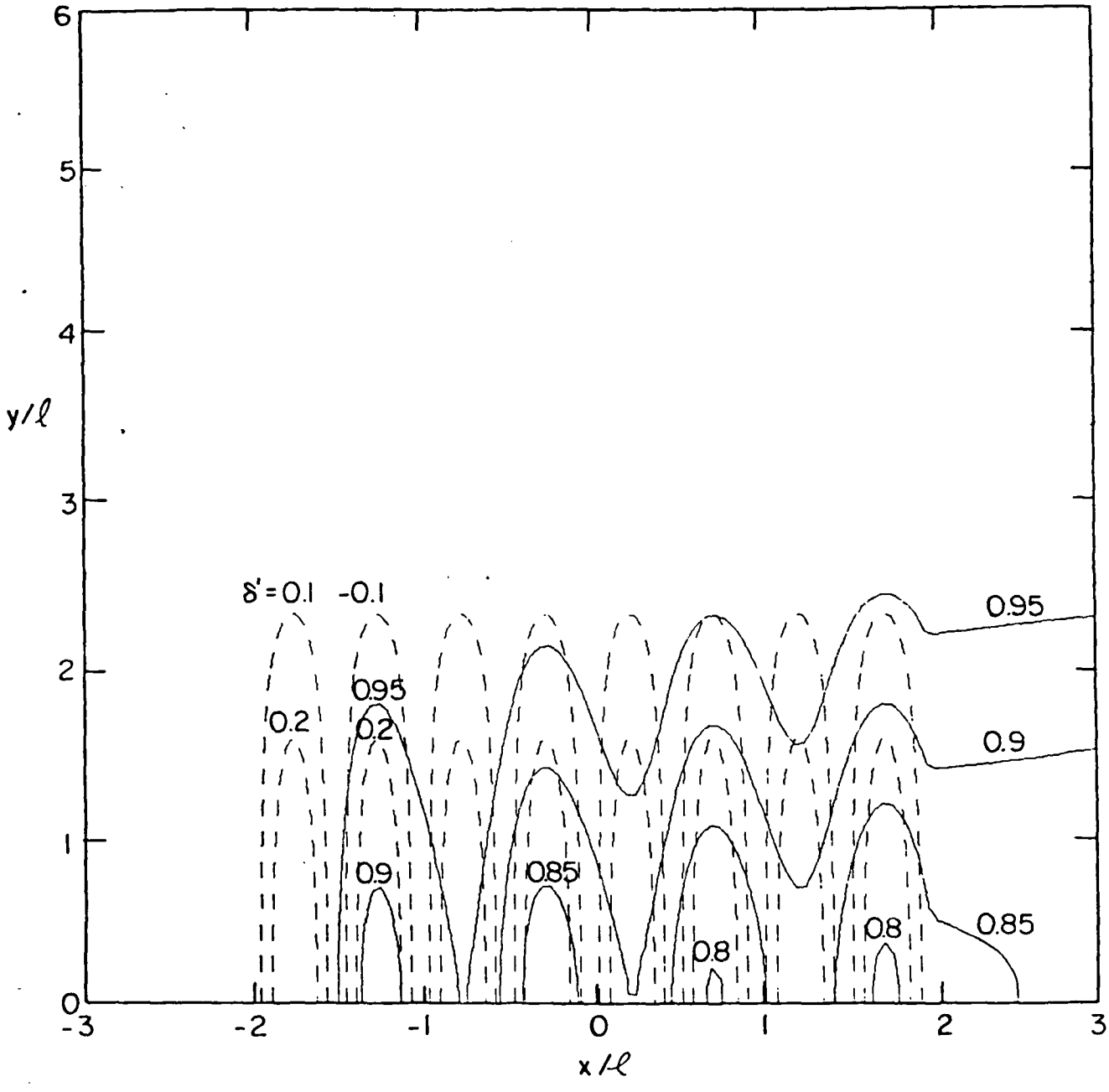

a) $|A|/A_o$

Figure III.7. Normalized amplitude contours: linear wave
—— amplitude contours; --- bottom contours
$\delta' = \delta/h_1$

dimensional patch of ripples of finite extent in the x and y directions. Ripples with length ℓ are aligned with crests parallel to the y-axis. The patch is symmetric about the x-axis with dimensions $n\ell x 2n\ell$ in x and y, where n is the number of ripples as before. The topography is specified according to Section II.4, equation (4.16). Computations were run with $2k/\lambda = 1$, $D/h_1 = 0.3$ and a farfield relative depth $kh_1 = 1$, giving $h_1 = \pi^{-1}$ with $\ell = 1$. The Ursell number $U_r = (a/h_1)/(kh_1)^2$ and wave steepness $\varepsilon = ka$ are thus both given by πA_0 for the incident wave.

Results were shown for the case of $n = 4$ in Figures III.7 and III.8. Figure III.7 gives results for the linear case, with normalized amplitude $|A/A_0|$ given in 7a, $|B/A_0|$ in 7b, and the total wave field in 7c. In Figure III.8, results are shown for the case of $\varepsilon = U_r = 0.2$. A comparison of the figures indicate some differences in the transmitted wave field over and downwave of the ripple patch, with the amplitude downwave of the last ripple being increased in the nonlinear case, indicating the greater tendency towards diffraction effects due to nonlinearity. This result is consistent with the phenomenon of self-defocussing as demonstrated by Kirby and Dalrymple (1983), and further is in agreement with Yue's (1980) results showing that diffraction of waves into a shadowed region proceeds more quickly in the nonlinear case. The reflected wave amplitudes are quite similar for both cases, with a minor increase in peak amplitude at the upwave end of the ripple patch being noted in the nonlinear case.

Comparisons of normalized amplitude for the total wave field along $y = 0$ and along $x = 3\ell$ are given in Figures III.9 a and b, respectively, for the linear and nonlinear cases. Differences are largely confined to a reduction in transmitted wave height downwave of the ripple patch in the nonlinear case, as discussed above.

$$\phi_1 = \frac{2ga}{\omega} \cos kx \cos \left\{\frac{kU}{C_g} x + \omega t\right\} \qquad (4.8)$$

which reduces to the usual stationary form at U→0. It is clear that the stationary component cos(kx) is unaffected by the presence of U; the relation between the wave envelope and topography is thus unaltered.

The effect of nonlinearity is thus limited to the lengthening of the incident wave (for small R) with respect to the topography at fixed ω (or k). For large $2k/\lambda$, the effect is a downshift of the maxima and minima of R which increases with increasing ε. It is remarked that, for large R, the incident waves may be shortened by nonlinearity; the shift in the pattern of R would then be expected to be towards higher values of $2k/\lambda$.

In the present example, the large reflection coefficient at the peak $2k/\lambda$ causes a significant weakening of the nonlinear dispersion in the incident wave on the upwave side of the ripple patch. Referring to Figure III.1, we see that a reflection coefficient of 0.6-0.7 would lead to an effective nonlinear parameter D* with values in the neighborhood of 0. Nonlinearity thus has little effect on the reflection process when reflection is strong; this is born out by the result of little or no shift in peak value or location of R for this example. This conclusion in partially supported by the experimental results of Davies and Heathershaw, who saw little or no effect of varying wave steepness on peak reflection, up to the point of breaking in the incident wave.

III.5 Two-dimensional Topography

In order to take advantage of the relatively strong reflections caused by the undulating topography studied in the previous chapter, we construct a two-

The curve for nonlinear reflection shown in Figure III.5 is for the case of no wave-induced current. It was found that the presence or absence of the wave-induced flow had no significant effect on the reflection process; the corresponding curve for reflection including mean flows is thus not included. This result may be partially explained by considering a simplified set of equations taken from (2.28 - 2.29);

$$iA_x - \frac{\omega U}{CC_g} A = 0 \tag{4.3}$$

$$iB_x - \frac{\omega U}{CC_g} B = 0 \tag{4.4}$$

where depth is constant and amplitude dispersion is neglected. The quantity U may represent the wave-induced return flow or a small flow $(<O(\mu))$ imposed by boundary conditions. Oscillatory solutions of constant amplitude are given by

$$\{A(x),\ B(x)\} = \{a,b\}e^{ik'x} \tag{4.5}$$

where

$$k' = - kU/C_g \tag{4.6}$$

so that

$$\phi_1^+ = \frac{-ig}{2\omega} ae^{i\left[k\left(1 - \frac{U}{C_g}\right) x - \omega t\right]} + c.c. \tag{4.7a}$$

$$\phi_1^- = \frac{-ig}{2\omega} be^{i\left[-k\left(1 + \frac{U}{C_g}\right) x - \omega t\right]} + c.c. \tag{4.7b}$$

For simplicity, b may be set equal to a; the resulting standing wave may be written as

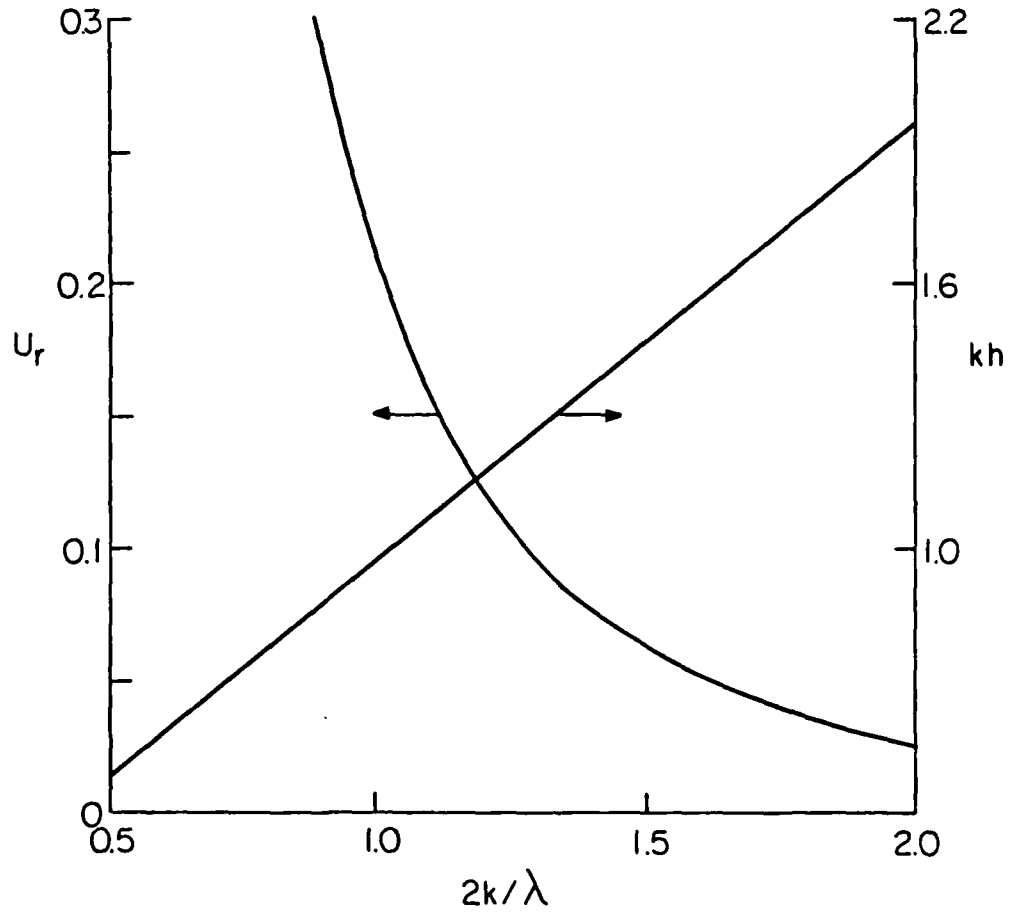

Figure III.6. Ursell number U_r for the nonlinear reflection example; $\varepsilon = 0.2$

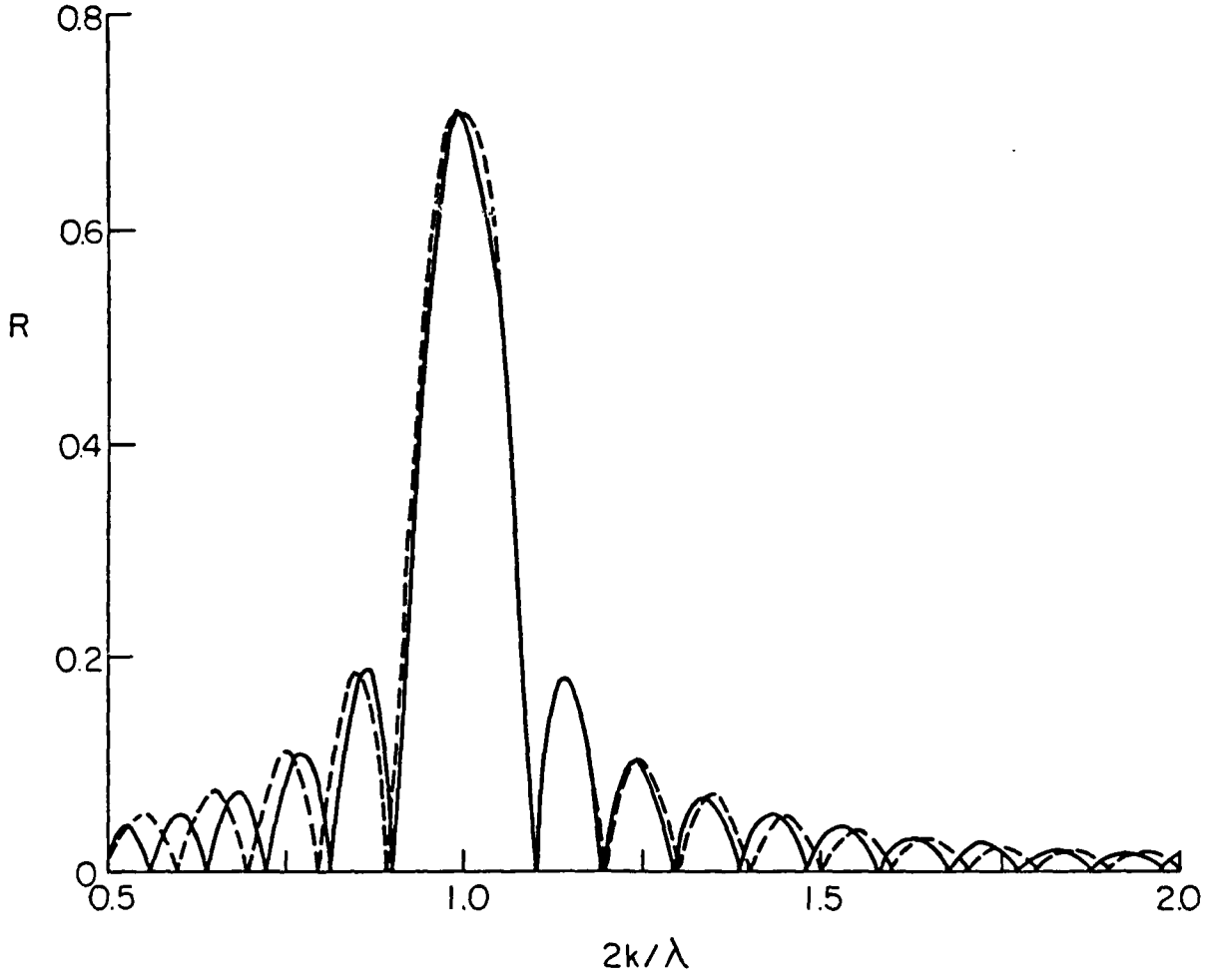

Figure III.5. Variation of R
n = 10, D/h_1 = 0.16
—— nonlinear, ε = 0.2, no current,
--- linear

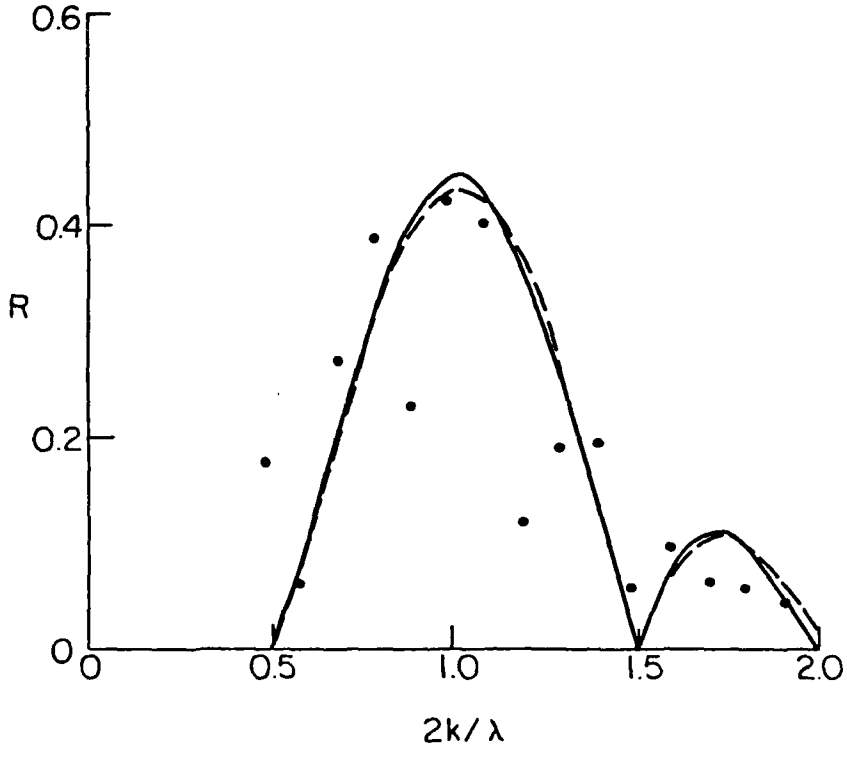

b) $D/h_1 = 0.32$, $n = 2$

Figure III.4. Continued

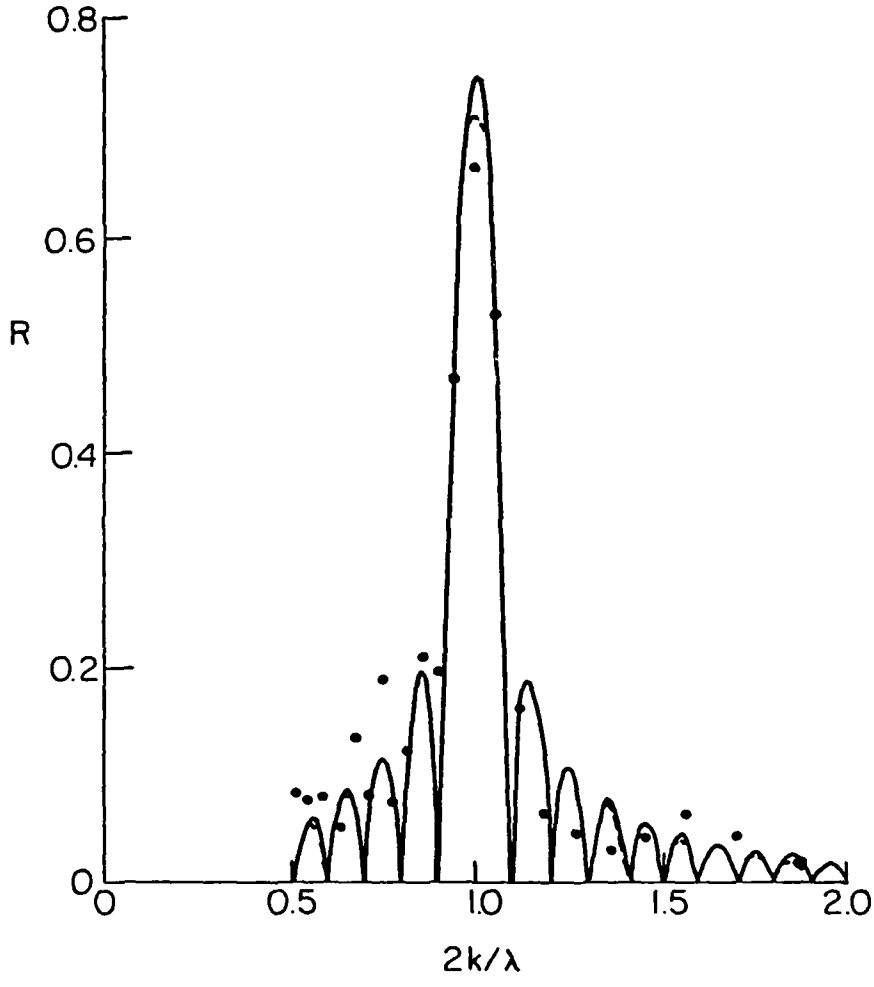

a) $D/h_1 = 0.16$, $n = 10$

Figure III.4. Comparison of coupled parabolic equations to full linear wave solution
—— linear solution, Davis and Heathershaw
--- coupled parabolic equations, $\Delta x = \lambda/20$
• Data, Davies and Heathershaw

In Chapter II, a numerical solution to the linearized elliptic problem was developed in order to compare to the analytic linear solution of Davies and Heathershaw (1984). The elliptic solution was shown to provide an accurate reproduction of the analytic results; comparisons with data were given above in Figures II.2 and II.3.

The theoretical results of Davies and Heathershaw were used as a check of the iterative scheme (3.12-13) in its linearized form. Results for the cases illustrated in Figures II.3 and II.4 were recomputed using the coupled parabolic equations, using a grid spacing $\Delta x=\ell/20$. The reflection coefficients for both cases are shown in Figure III.4. The peak reflection coefficients R obtained using the parabolic model are slightly less than the values predicted by the corrected theory of Davies and Heathershaw. For $2k/\lambda>2.0$ the number of points per incident wavelength drops below 20, and some reduction in the reflection coefficient was noted. A further reduction in grid spacing to $\Delta x=\ell/10$ caused a reduction of the reflected wave amplitude at $2k/\lambda=1$ of 6.6% for the case with n=10. Therefore, the value of $\Delta x=\ell/20$ was used for all subsequent runs.

We now use the nonlinear form of the parabolic equation to study the reflection process. Tests were performed using the geometry of Figure III.4a ($D/h_1 = 0.16$); results are presented in Figure III.5 for incident wave steepness $\varepsilon = kA_0 = 0.2$. A plot of Ursell number $U_r = (A_0/h)/(kh)^2$ for this case is given in Figure III.6. The plot indicates that, for the chosen value of ε, results of the Stokes wave model are only roughly valid for the region $2k/\lambda<1$. For small values of $2k/\lambda$ (large wavelength) it is anticipated that the incident wave phase speed is overestimated. This would have the effect of over emphasizing the differences between the linear and nonlinear reflection curves in this range.

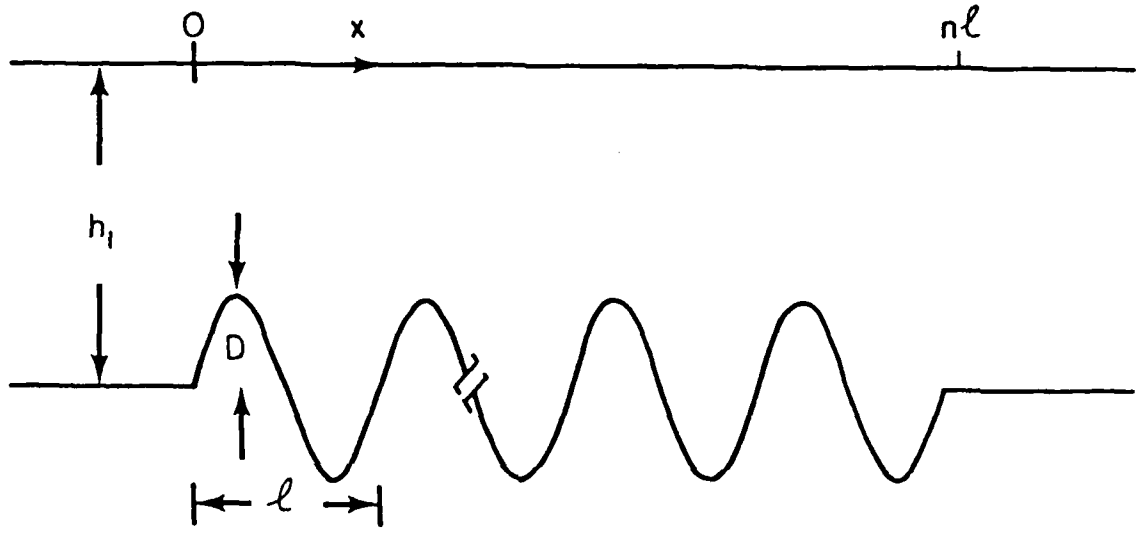

Figure III.3 Topography for one-dimensional model tests

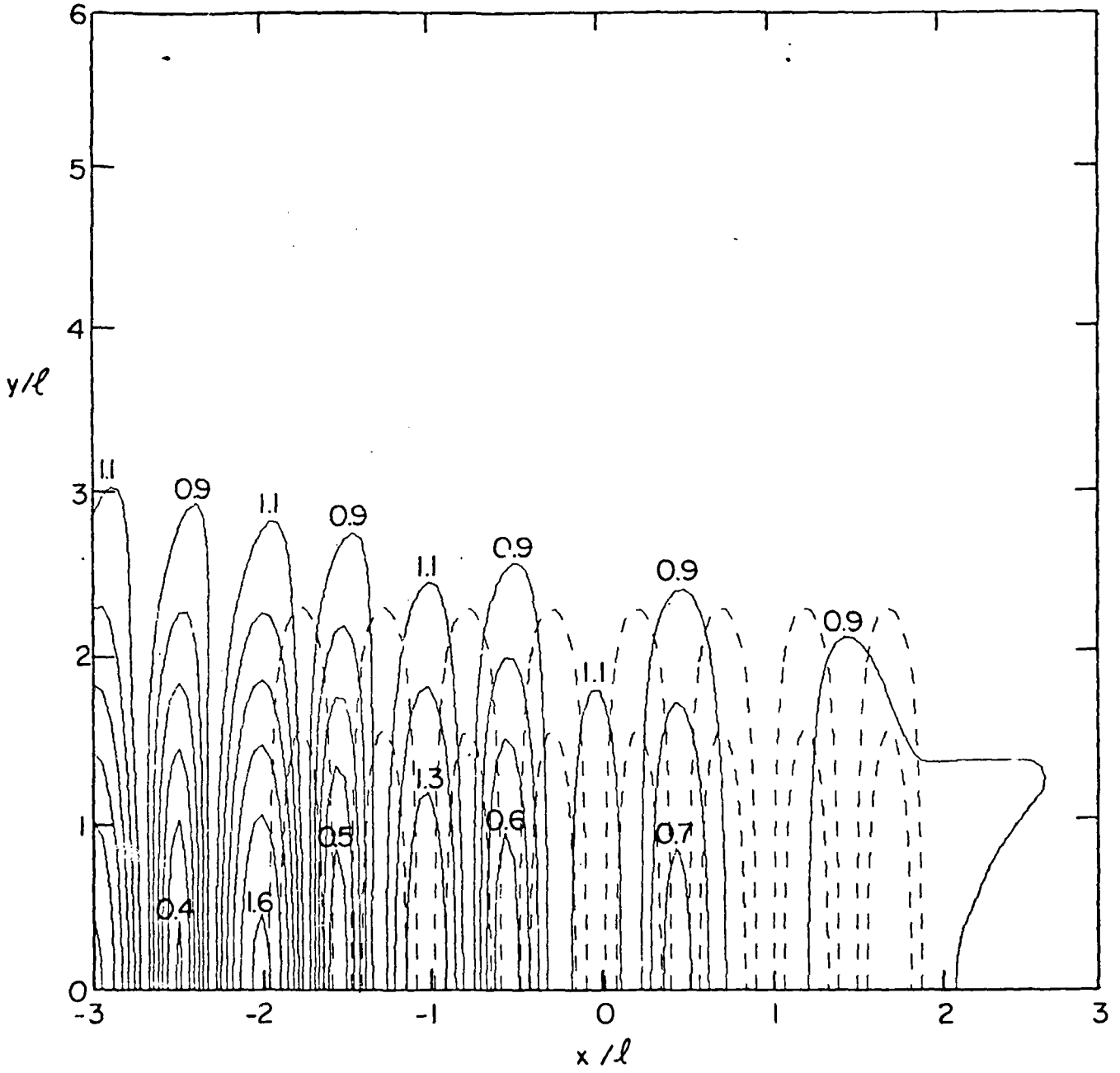

c) $|\eta|/A_o$

Figure III.8. Continued

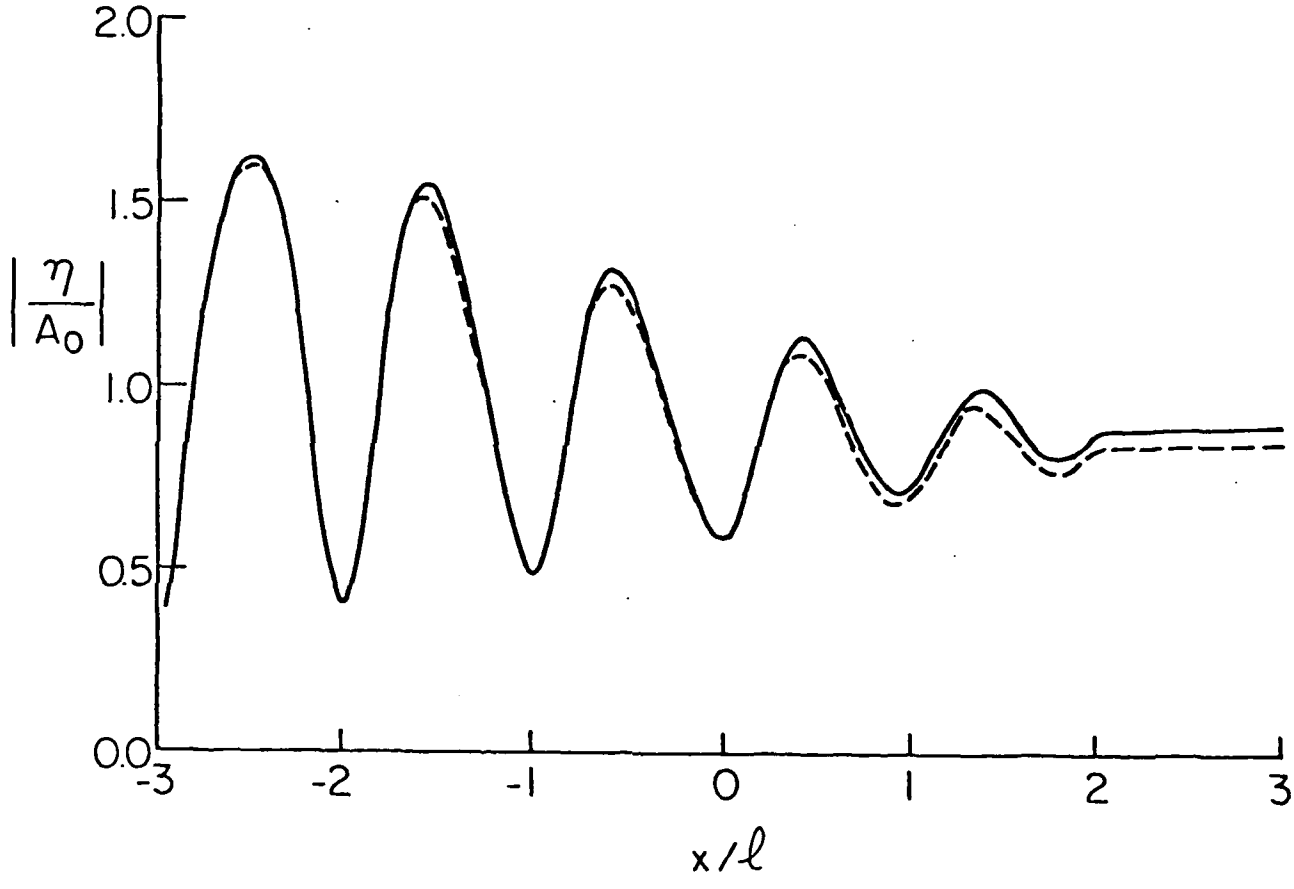

a) Amplitude along centerline y = 0

Figure III.9. Amplitude $|\eta|/A_o$ for ripple patch.
n = 4, $D/h_1 = 0.3$, $h_1 = \pi^{-1}$
—— nonlinear waves, $\varepsilon = 0.2$;
--- linear waves

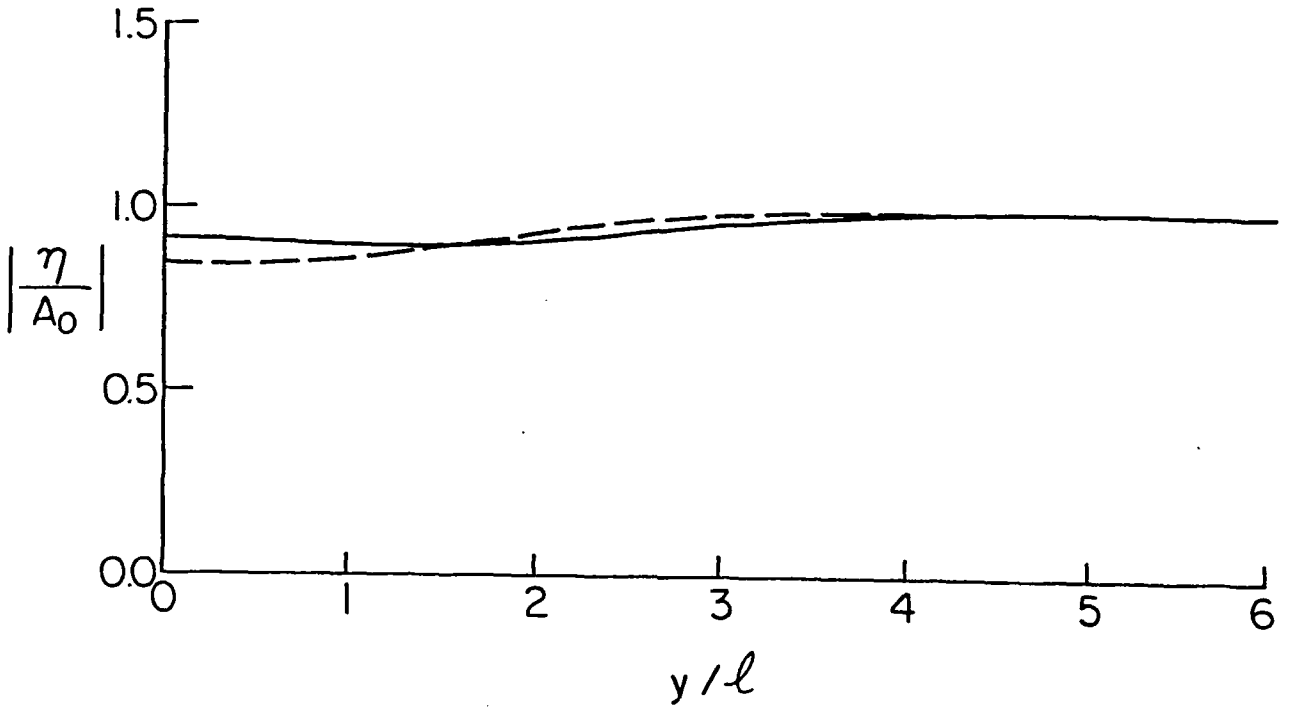

b) Amplitude along downwave transect $x/\ell = 3$

Figure III.9. Continued

The effect of diffraction in the present example may be estimated simply. If we take the peak reflection along the centerline to be approximately R = 0.6 from Figures 7 or 8 b), we conclude that the transmitted amplitude downwave of the patch should be

$$T = (1-R^2)^{1/2} = 0.8$$

This value is in rough agreement with the linear result but underestimates the nonlinear value of $T \tilde{=} 0.9$, again indicating the more rapid effects of diffraction in the nonlinear case.

III.6 Discussion

In this study we have utilized a variational principal to develop a wave equation governing the propagation of Stokes waves in a varying domain, after which use is made of a splitting method to provide coupled equations for forward and back-scattered components of an initially plane incident wave propagating over uneven topography.

The restriction to Stokes waves and the resulting constraints on water depth relative to the incident wavelength made it difficult to develop computational examples which describe a significant reflection process arising over a short spatial scale. Under the mild-slope conditions, it is likely that the gradual reflection process would be apparent over only fairly long spatial scales. For the case of shallower water, the Stokes wave formulation is no longer valid, and recourse must be made to appropriate equations such as the Boussinesq equations. The parabolic approximation for a spectrum of steady (in time) forward-scattered waves in the shallow water regime has been provided by Liu, Yoon and Kirby (1985); the development of a model for partial

reflection in this case will be the subject of a further investigation. Also of special interest is the case where the incident wave amplitude is modulated in space and time. The treatment of "groupy" waves is not approachable using the reduced wave equation of Section III.3; however, the general time dependent model (2.15) may form the basis of such an approach, after further accounting for terms arising due to possible fast modulations of $O(\varepsilon)$ in the amplitude functions.

Appendix III.A Integrals of f functions

The integrals I are defined as the integral over total depth of an integrand f, and may be expanded according to

$$I = \int_{-h}^{\eta} f\,dz = \int_{-h}^{o} f\,dz + \eta f|_o + \eta^2 \frac{f_z|_o}{2} + \eta^3 \frac{f_{zz}|_o}{6} + \ldots$$

$$= I' + \eta I'' + \eta^2 I''' + \eta^3 I'^{v} + \ldots \qquad (A.1)$$

Substitution of the expansion (2.4b) for η yields (2.7). The individual integrals and required components are given by

$$I_1 = \int_{-h}^{\eta} f_1 dz \quad ; \quad I_1'' = 1,\ I_1''' = \omega^2/2g,\ I_1'^{v} = k^2/6 \qquad (A.2)$$

$$I_{1,1} = \int_{-h}^{\eta} f_1^2\, dz \quad ; \quad I'_{1,1} = CC_g/g,\ I''_{1,1} = 1,\ I'''_{1,1} = \omega^2/g \qquad (A.3)$$

$$I^z_{1,1} = \int_{-h}^{\eta} f_{1_z}^2\, dz \quad ; \quad I^{z'}_{1,1} = (\omega^2 - k^2 CC_g)/g,\ I^{z''}_{1,1} = \omega^4/g^2,\ I^{z'''}_{1,1} = k^2\omega^2/g \qquad (A.4)$$

$$I_2 = \int_{-h}^{\eta} f_2 dz \ ; \ I_2' = \frac{\cosh kh}{k\sinh^3 kh}\ ,\ I_2'' = \frac{\cosh 2kh}{\sinh^4 kh}\ ,\ I_2''' = \frac{2k\cosh kh}{\sinh^3 kh} \qquad (A.5)$$

$$I_{1,2} = \int_{-h}^{\eta} f_1 f_2 dz \ ; \ I''_{1,2} = \frac{\cosh 2kh}{\sinh^4 kh} \qquad (A.6)$$

$$I^{z}_{1,2} = \int_{-h}^{\eta} f_{1_z} f_{2_z} \; ; \; I^{z''}_{1,2} = 4k^2/\sinh^2 kh \tag{A.7}$$

$$I_{2,2} = \int_{-h}^{\eta} f_2^2 dz \quad ; \quad I'_{2,2} = \frac{\sinh 2kh}{2k\sinh^8 kh} \{\sinh^2 kh + C_g/C\} \tag{A.8}$$

$$I^{z}_{2,2} = \int_{-h}^{\eta} f_{2_z}^2 dz \; ; \; I^{z'}_{2,2} = \frac{2k\sinh 2kh}{\sinh^8 kh} \{\cosh^2 kh - C_g/C\} \tag{A.9}$$

Appendix III.B Components of the primitive Lagrangian L

The Lagrangian L is expanded as a series in powers of the wave steepness parameter ε without regard to the relative size of the modulation parameter μ. After expanding η and the integrals I in (2.6), the individual components of L in (2.8) are given by (after dividing out the constant density ρ)

$$L_o = \frac{-gh^2}{2} \qquad ; \qquad L_1 = I_1' \tilde{\phi}_{1_t} \tag{B.1,2}$$

$$L_2 = \frac{g\eta_1^2}{2} + I_1''\eta_1\tilde{\phi}_{1_t} + I_{1,1}' \frac{(\nabla_h\tilde{\phi}_1)^2}{2} + I_{1,1}^{z'} \frac{(\tilde{\phi}_1)^2}{2} + h(\phi_{2_t}' - \gamma_2) + I_2'\tilde{\phi}_{2_t}$$

(B.3)

$$L_3 = g\eta_1(\eta^2 + b_2) + I_1'' (\eta_2 + b_2)\tilde{\phi}_{1_t} + I_1''' \eta_1^2\tilde{\phi}_{1_t} + \eta_1(\phi_{2_t}' - \gamma_2)$$

$$+ I_2''\eta_1\tilde{\phi}_{2_t} + I_{1,1}'' \eta_1 \frac{(\nabla_h\tilde{\phi}_1)^2}{2} + I_{1,2}'\nabla_h\phi_1\cdot\nabla_h\tilde{\phi}_2 + I_1' \nabla_h\tilde{\phi}_1\cdot\nabla_h\phi_2'$$

$$+ I_{1,1}^{z''} \frac{\eta_1\tilde{\phi}_1^2}{2} + I_{1,2}^{z'} \tilde{\phi}_1\tilde{\phi}_2 \tag{B.4}$$

$$L_4 = \frac{g(\eta_2 + b_2)^2}{2} + (\eta_2 + b_2)\phi_{2_t}' + 2I_1'''\eta_1\,(\eta_2 + b_2)\tilde{\phi}_{1_t} + I_1^{'v}\eta_1^3\tilde{\phi}_{1_t}$$

$$+ I_2''(\eta_2 + b_2)\tilde{\phi}_{2_t} + I_2'''\,\eta_1^2\,\tilde{\phi}_{2_t} + I_{1,1}''(\eta_2 + b_2)\,\frac{(\nabla_h\tilde{\phi}_1)^2}{2}$$

$$+ I_{1,1}''\eta_1^2\,\frac{(\nabla_h\tilde{\phi}_1)^2}{2} + I_{2,2}'\,\frac{(\nabla_h\tilde{\phi}_2)^2}{2} + h\,\frac{(\nabla_h\phi_2')^2}{2} + I_{1,2}'\eta_1\nabla_h\tilde{\phi}_1\cdot\nabla_h\tilde{\phi}_2$$

$$+ \eta_1\nabla_h\tilde{\phi}_1\cdot\nabla_h\phi_2' + I_2'\nabla_h\tilde{\phi}_2\cdot\nabla_h\phi_2' + I_{1,1}^{z''}\,(\eta_2 + b_2)\,\frac{(\tilde{\phi}_1)^2}{2} + I_{1,1}^{z'''}\,\eta_1^2\,\frac{\tilde{\phi}_1^2}{2}$$

$$+ I_{2,2}^{z'}\,\frac{(\tilde{\phi}_2)^2}{2} + I_{1,2}^{z''}\,\eta_1\tilde{\phi}_1\tilde{\phi}_2 - \gamma_2(\eta_2 + b_2) \qquad \text{(B.5)}$$

Appendix III.C. General Form for $O(\varepsilon^3)$ term in wave equation

The term {N.L.T.} in (2.15) is given here in terms of $\tilde{\phi}_1, \tilde{\phi}_2$, $(\eta_2 + b_2)$ and ϕ_2'. The first order surface η_1 has been eliminated through use of (2.9). Further, we have made use of the fact that

$$(\tilde{\phi}_1, \tilde{\phi}_2)_{tt} = (-\omega^2\tilde{\phi}_1, -4\omega^2\tilde{\phi}_2) + O(\mu) \tag{C.1}$$

$$\nabla_h^2(\tilde{\phi}_1, \tilde{\phi}_2) = (-k^2\tilde{\phi}_1, -4k^2\tilde{\phi}_2) + O(\mu) \tag{C.2}$$

for both progressive and standing waves. {N.L.T.} is then given by

$$\begin{aligned}
\{\text{N.L.T.}\} = \Big\{ & \frac{-gk^2}{\cosh^2 kh}(\eta_2 + b_2) + \frac{2\omega^2k^2}{g^2}(\tilde{\phi}_{1_t})^2 - k^4\tanh^2 kh(\tilde{\phi}_1)^2 \\
& -k^2\tanh^2 kh\,(\nabla_h\tilde{\phi}_1)^2 - \frac{8k^2}{\sinh^2 kh}\tilde{\phi}_{2_t}\Big\}\tilde{\phi}_1 \\
& + \Big\{-2k\,\tanh khn_{2_t} + \frac{4k^2(1 - 2\sinh^2 kh)}{\sinh^4 kh}\tilde{\phi}_2 \\
& + \frac{k\tanh kh}{g}(\nabla_h\tilde{\phi}_1)_t^2\Big\}\tilde{\phi}_{1_t} \\
& + \Big\{g\nabla_h(\eta_2 + b_2) + \frac{k\tanh kh}{g}\nabla_h(\tilde{\phi}_{1_t}^2) - \frac{\cosh 2kh}{\sinh^4 kh}\nabla_h\tilde{\phi}_{2_t}\Big\}\cdot\nabla_h\tilde{\phi}_1 \\
& + \Big\{-2\nabla_h\phi_2' - \frac{2\cosh 2kh}{\sinh^4 kh}\nabla_h\tilde{\phi}_2\Big\}\cdot\nabla_h\tilde{\phi}_{1_t} \quad ,
\end{aligned} \tag{C.3}$$

where we have substituted for all I values from Appendix III.A.

REFERENCES

Benney, D.J., 1962, "Nonlinear gravity wave interactions," J. Fluid Mech., 14: 577-584.

Berkhoff, J.C.W., 1972, "Computation of combined refraction-diffraction", Proc. 13th Int. Conf. Coastal Engineering, Vancouver.

Berkhoff, J.C.W., Booij, N., and Radder, A.C., 1982, "Verification of numerical wave propagation models for simple harmonic linear waves," Coastal Engineering, 6: 255-279.

Chu, V.H. and Mei, C.C., 1970, "On slowly varying Stokes waves," J. Fluid Mech., 41, 873-887.

Corones, J., 1975, Bremmer series that correct parabolic approximations. J. Math. Anal. Applic., 50: 361-372.

Dalrymple, R.A. and Kirby, J.T., 1984, "Water waves over ripples," submitted to J. Waterway Port Coastal and Ocean Engrng.

Davies, A.G. and Heathershaw, A.D., 1983, "Surface wave propagation over sinusoidally varying topography: theory and observation," Report 159, Institute of Oceanographic Sciences, 181 pp.

Davies, A.G. and Heathershaw, A.D., 1984, "Surface-wave propagation over sinusoidally varying topography", J. Fluid Mech., 144, 419-443.

Djordjevic, V.D. and Redekopp, L.G., 1978, "On the development of packets of surface gravity waves moving over an uneven bottom," Z.A.M.P., 29, 950-960.

Dolan, T.J., 1983, "Wave mechanisms for the formation of multiple longshore bars with emphasis on the Chesapeake Bay," M.S. Thesis, Dept. of Civil Engineering, University of Delaware.

Dysthe, K.B., 1974, "A note on the application of Whitham's method to nonlinear waves in dispersive media," J. Plasma Phys., 11: 63-76.

Heathershaw, A.D., 1982, "Seabed-wave resonance and sand bar growth", Nature 296, 343-345.

Kirby, J.T., 1983, "Propagation of weakly-nonlinear surface water waves in regions with varying depth and current," Ph.D. dissertation, University of Delaware, Newark.

Kirby, J.T., 1984, "A note on linear surface wave-current interaction over slowly varying topography", J. Geophys. Res., 89, 745-747.

Kirby, J.T., Dalrymple, R.A. and Liu, P.L-F., 1981, "Modification of edge waves by barred beach topography", Coastal Engineering, 5, 35-49.

Kirby, J.T. and Dalrymple, R.A., 1983a, "Propagation of obliquely incident water waves over a trench," J. Fluid Mech., 133, 47-63.

Kirby, J.T. and Dalrymple, R.A., 1983b, "A parabolic equation for the combined refraction-diffraction of Stokes waves by mildly varying topography," J. Fluid Mech., 136: 543-566.

Kirby, J.T. and Dalrymple, R.A., 1984, "Verification of a parabolic equation for propagation of weakly-nonlinear waves," Coastal Engineering, 8, 219-232.

Kirby, J.T. and Dalrymple, R.A., 1984, "Propagation of weakly-nonlinear surface waves in regions with varying depth and current," in preparation.

Liu, P.L-F., 1983, "Wave-current interactions on a slowly varying topography", J. Geophys. Res., 88, 4421-4426.

Liu, P.L.-F. and Mei, C.C., 1976, "Water motion on a beach in the presence of a breakwater. 1. Waves," J. Geophys. Res., 81: 3079-3094.

Liu, P.L-F. and Tsay, T-K., 1983, "On weak reflection of water waves", J. Fluid Mech., 131, 59-71.

Liu, P.L.-F. and Tsay, T.-K., 1984, "Refraction-diffraction model for weakly-nonlinear water-waves," J. Fluid Mech., 141: 265-274.

Liu, P.L.-F., Yoon, S.B. and Kirby, J.T., 1985, "Nonlinear refraction-diffraction of waves in shallow water," J. Fluid Mech., in press.

Lozano, C.J., 1977, "Gravity surface waves on waters of variable depth," unpublished manuscript.

Luke, J.C., 1967, "A variational principle for a fluid with a free surface," J. Fluid Mech., 27: 395-397.

McDaniel, S.T., 1975, Parabolic approximations for underwater sound propagation, J. Acoust. Soc. Am., 58: 1178-1185.

McIver, P. and Evans, D.V., 1984, "The trapping of surface waves above a submerged, horizontal cylinder", submitted to J. Fluid Mech.

Mei, C.C., 1983, The Applied Dynamics of Ocean Surface Waves, John Wiley and Sons, New York.

Mei, C.C., 1985, "Resonant reflection of surface water waves by periodic sand bars", J. Fluid Mech., in press.

Radder, A.C., 1979, "On the parabolic equation method for water wave propagation", J. Fluid Mech., 95, 159-176.

Roskes, G.J., 1976, "Nonlinear multiphase deep-water wavetrains," Phys. Fluids, 19, (8) 1253-1254.

Smith, R. and Sprinks, T., 1975, "Scattering of surface waves by a conical island", J. Fluid Mech., 72, 373-384.

Symonds, G. and Bowen, A.J., 1984, "Interactions of nearshore bars with incoming wave groups", J. Geophys. Res., 89, 1953-1959.

Symonds, G., Huntley, D.A. and Bowen, A.J., 1982, "Two-dimensional surf beat: long wave generation by a time-varying breakpoint", J. Geophys. Res., 87, 492-498.

Tsay, T.-K. and Liu, P.L.-F., 1982, Numerical solution of water-wave refraction and diffraction problems in the parabolic approximation, J. Geophys. Res., 87: 7932-7940.

Tsay, T.-K. and Liu, P.L.-F., 1983, A finite element model for wave refraction and diffraction, Appl. Ocean Res., 5: 30-37.

Whitham, G.B., 1967, "Non-linear dispersion of water waves," J. Fluid Mech., 27: 399-412.

Yue, D.K.-P., 1980, "Numerical study of Stokes wave diffraction at grazing incidence," Sc.D. dissertation, Massachusetts Institute of Technology.

Distribution

ffice of Naval Research
oastal Science Program
ode 42205
rlington, VA 22217

efense Documentation Center
ameron Station
lexandria, VA 22314

irector, Naval Research Lab.
TTN: Technical Information Officer
ashington, D. C. 20375

irector
ffice of Naval Research Branch Office
030 East Green Street
asadena, CA 91101

hief of Naval Research
ode 100M
ffice of Naval Research
rlington, VA 22217

ffice of Naval Research
perational Applications Division
ode 200
rlington, VA 22217

ffice of Naval Research
cientific Liaison Officer
cripps Institution of Oceanography
a Jolla, CA 92093

irector Naval Research Laboratory
TTN: Library, Code 2628
ashington, D. C. 20375

NR Scientific Liaison Group
merican Embassy - Room A-407
PO San Francisco, CA 96503

ommander
aval Oceanographic Office
TTN: Library, Code 1600
ashington, D. C. 20374

aval Oceanographic Office
ode 3001
ashington, D. C. 20374

Chief of Naval Operations
OP 987P1
Department of the Navy
Washington, D. C. 20350

Oceanographer of the Navy
Hoffman II Building
200 Stovall Street
Alexandria, VA 22322

Naval Academy Library
U. S. Naval Academy
Annapolis, MD 21402

Commanding Officer
Naval Coastal Systems Laboratory
Panama City, FL 32401

Director
Coastal Engineering Research Center
U. S. Army Corps of Engineers
Kingman Building
Fort Belvoir, VA 22060

Officer in Charge
Environmental Research Prodctn Felty.
Naval Postgraduate School
Monterey, CA 93940

Director
Amphibious Warfare Board
U. S. Atlantic Fleet
Naval Amphibious Base
Norfolk, Little Creek, VA 23520

Commander, Amphibious Force
U. S. Pacific Fleet
Force Meteorologist
Comphibpac Code 25 5
San Diego, CA 93155

Librarian, Naval Intelligence
Support Center
4301 Suitland Road
Washington, D. C. 20390

Commanding Officer
Naval Civil Engineering Laboratory
Port Hueneme, CA 93041